AD ________________

Award Number: DAMD17-98-1-8210

TITLE: Development of a Digital Stereoscopic Imaging Technique in Mammography

PRINCIPAL INVESTIGATOR: Heang-Ping Chan, Ph.D.

CONTRACTING ORGANIZATION: University of Michigan
Ann Arbor, Michigan 48109-1274

REPORT DATE: May 2003

TYPE OF REPORT: Final

PREPARED FOR: U.S. Army Medical Research and Materiel Command
Fort Detrick, Maryland 21702-5012

DISTRIBUTION STATEMENT: Approved for Public Release;
Distribution Unlimited

The views, opinions and/or findings contained in this report are those of the author(s) and should not be construed as an official Department of the Army position, policy or decision unless so designated by other documentation.

20030923 071

REPORT DOCUMENTATION PAGE

Form Approved
OMB No. 074-0188

Public reporting burden for this collection of information is estimated to average 1 hour per response, including the time for reviewing instructions, searching existing data sources, gathering and maintaining the data needed, and completing and reviewing this collection of information. Send comments regarding this burden estimate or any other aspect of this collection of information, including suggestions for reducing this burden to Washington Headquarters Services, Directorate for Information Operations and Reports, 1215 Jefferson Davis Highway, Suite 1204, Arlington, VA 22202-4302, and to the Office of Management and Budget, Paperwork Reduction Project (0704-0188), Washington, DC 20503

1. AGENCY USE ONLY (Leave blank)	2. REPORT DATE	3. REPORT TYPE AND DATES COVERED
	May 2003	Final (20 Apr 98 - 19 Apr 03)

4. TITLE AND SUBTITLE
Development of a Digital Stereoscopic Imaging Technique in Mammography

5. FUNDING NUMBERS
DAMD17-98-1-8210

6. AUTHOR(S)
Heang-Ping Chan, Ph.D.

7. PERFORMING ORGANIZATION NAME(S) AND ADDRESS(ES)
University of Michigan
Ann Arbor, Michigan 48109-1274

E-MAIL: chanhp@umich.edu

8. PERFORMING ORGANIZATION REPORT NUMBER

9. SPONSORING / MONITORING AGENCY NAME(S) AND ADDRESS(ES)
U.S. Army Medical Research and Materiel Command
Fort Detrick, Maryland 21702-5012

10. SPONSORING / MONITORING AGENCY REPORT NUMBER

11. SUPPLEMENTARY NOTES

12a. DISTRIBUTION / AVAILABILITY STATEMENT
Approved for Public Release; Distribution Unlimited

12b. DISTRIBUTION CODE

13. ABSTRACT ***(Maximum 200 Words)***

The goal of this research is to develop stereoscopic techniques for mammographic imaging and to investigate the feasibility of using stereomammography to improve the sensitivity of mammography for breast cancer diagnosis.

During the project years, we have performed extensive investigation of the effects of image acquisition techniques including stereo shift, exposure, and geometric magnification on the depth discrimination capability of digital stereomammography. Software tools have been developed for two high-resolution stereo display workstations The software allows manipulation of the displayed images and provides 3D virtual cursors for the measurement of the depth of a lesion in the image. Observer experiments have been performed to evaluate the stereomammography imaging technique using stereo images of a specially designed 3D modular phantom. A database of stereo images of biopsied breast tissue specimens was collected and observer performance experiments were conducted to compare the accuracy of lesion characterization and margin clearance identification on stereoscopic and monoscopic images. A pilot study was performed to compare radiologists' impressions of full field digital stereomammograms with conventional mammograms obtained from informed consent breast cancer patients. The results of this project indicate that stereomammography is technologically feasible and it is a promising technique that will provide additional 3D information for the detection and characterization of breast lesions. Further studies are therefore warranted to investigate whether stereomammography can improve the sensitivity of mammography for breast cancer detection, especially in dense breasts.

14. SUBJECT TERMS
mammography, stereoscopic imaging, depth perception, breast cancer diagnosis

15. NUMBER OF PAGES
78

16. PRICE CODE

17. SECURITY CLASSIFICATION OF REPORT	18. SECURITY CLASSIFICATION OF THIS PAGE	19. SECURITY CLASSIFICATION OF ABSTRACT	20. LIMITATION OF ABSTRACT
Unclassified	Unclassified	Unclassified	Unlimited

NSN 7540-01-280-5500

Standard Form 298 (Rev. 2-89)
Prescribed by ANSI Std. Z39-18
298-102

(3) Table of Contents

(4) Introduction

The goal of this project is to develop a digital stereoscopic imaging technique for mammography. We hypothesize that stereoscopic imaging can be a practical technique with current detector and display technology, and stereoscopic imaging will improve the detection and analysis of breast lesions, especially for dense breasts. The improvement results from the facts that: (1) digital imaging systems generally can provide better contrast sensitivity for imaging dense tissues, (2) the over- and underlying dense tissues will be separated from the lesion in the stereoscopic views thereby increasing the conspicuity of the lesion, and (3) the ability to analyze the 3-dimensional distributions and shapes of lesions such as calcifications and masses within the breast can potentially improve the accuracy of mammographic image interpretation by radiologists and reduce unnecessary biopsies.

To accomplish this goal, we first performed phantom studies to develop an optimal imaging technique for the acquisition of the stereoscopic images. This included the determination of the stereoscopic angle, the magnification factor, and the dose requirements in comparison with those for a single-image technique. To view the digital stereoscopic images, we developed a stereoscopic viewing station with a high-resolution stereo graphics board and monitor. We also developed and implemented software for panning and roaming the displayed images and for adjusting the contrast and brightness of the images. A stereoscopic viewer with an LCD shutter is used to separate the left eye and right eye images. Any one image of the stereoscopic pair can also be viewed independently as in a conventional single-image reading condition. The stereomammography imaging technique was evaluated with an observer performance experiment in which the accuracies of experienced radiologists in characterizing lesions and in determining margin clearance were compared for readings of mono and stereo images of biopsy tissue samples.

In the course of the research, we also developed a new idea of using a virtual cursor for absolute depth measurements of objects in stereo images. A series of observer experiments with phantom images was performed to demonstrate the usefulness and evaluate the accuracies of depth measurement using virtual cursors.

In summary, we performed an extensive investigation of the dependence of the accuracies of depth discrimination and depth measurement on image acquisition techniques in digital stereomammography. We also developed software tools for the manipulation of the displayed stereo images and for the measurement of the depth of a lesion in the images. These tools were developed for two different stereo display workstations. Observer experiments were performed to evaluate the stereomammography imaging technique using phantoms and biopsied breast tissue samples. The results indicate that stereoscopic imaging is a promising technique that may provide 3D information for the detection and characterization of breast lesions. Further studies are warranted to investigate whether stereomammography can improve the sensitivity of mammography for breast cancer detection, especially in dense breasts.

(5) Body

This is the final report of our project. In the project period (4/20/98-4/19/03), we have performed a number of studies to develop the digital stereoscopic imaging technique. The detailed studies and results have been reported previously in the annual progress reports. A summary of some of the important accomplishments follows.

(A) Development of Stereo Display Workstations and Graphical User Interface

Since there is no high-resolution stereo workstation commercially available for the display of digital stereomammograms, we had to work with manufacturers of high quality medical image displays to develop appropriate displays of the stereomammograms obtained in this project. Two stereo display workstations were developed in the course of this study:

(1) Barco-Metheus SUN-based stereo display workstation

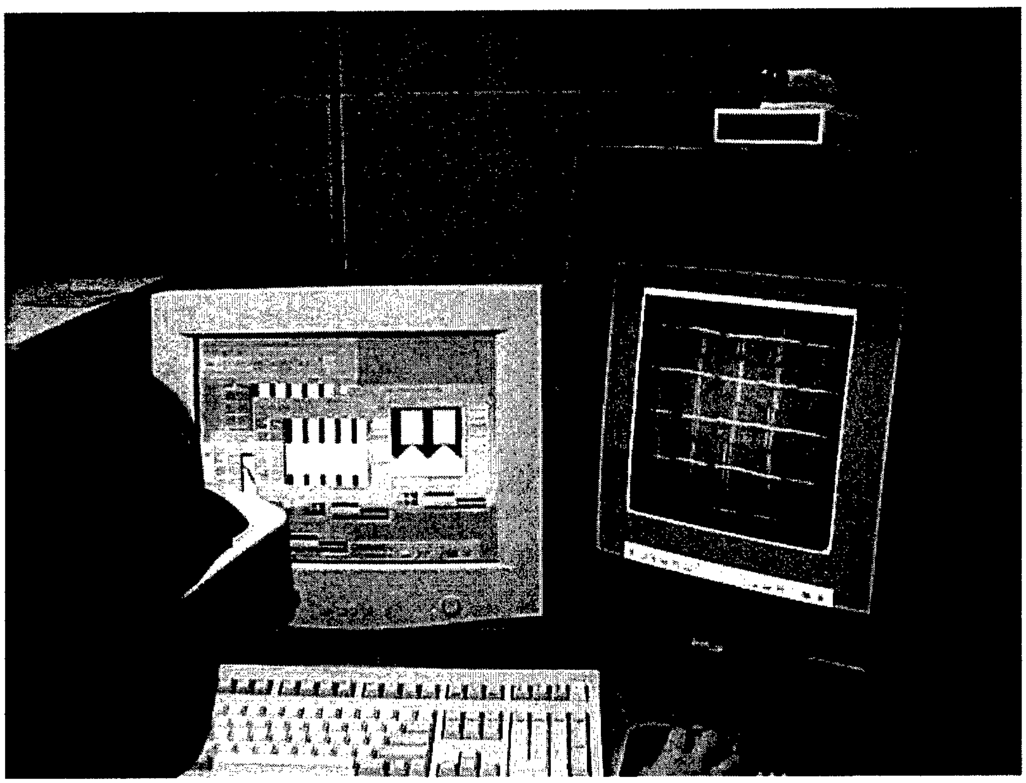

Figure 1. Barco-Metheus SUN-based stereoscopic display workstation.

The first system that we acquired consists of a model 1760S Barco-Metheus (Beaverton, OR) stereoscopic graphics board in a SUN Microsystems (Palo Alto, CA) Ultra 10 computer that drives a Barco model 521 (5 Megapixel) 21"stereo display monitor. The Barco-Metheus graphics board displays 1408 x 1408 x 8 bit images at a refresh rate of 114 Hz. It operates in a page flipping stereoscopic mode with the left- and right-eye images displayed alternately. NuVision (Beaverton, OR) LCD stereoscopic glasses were used for viewing the stereoscopic images. We chose this system because it was the only high-resolution stereo display system available at a reasonable price at that time. In addition, we originally planned to acquire stereo images with a Fischer core biopsy digital unit that has a 1024 X 1024 image matrix size so that the display resolution was adequate. The stereo workstation is shown in Fig. 1. We have developed image manipulation software such as windowing, zooming, panning, and a number of virtual cursors for the workstation. All phantom experiments were conducted using this display.

(2) Dome-MegaScan PC based Stereo Display Workstation

In the summer of 2000, our department purchased the first commercially available full field digital mammography (FFDM) system by General Electric Medical System (Senographe 2000D; Milwaukee, WI) for the breast imaging clinic. Because the FFDM system had greater potential for future clinical applications than the small (5 cm x 5 cm) field Fischer core biopsy unit, we decided to employ the FFDM system for the acquisition of digital stereo mammograms for our project. The matrix size of the FFDM images is about 2300 x 1900. However, the Metheus-Barco system can only display 1408 x 1408 stereo images at a 114 Hz refresh rate. It therefore cannot display the entire full field stereomammogram at once, and requires the use of panning for the visualization of all parts of the mammograms.

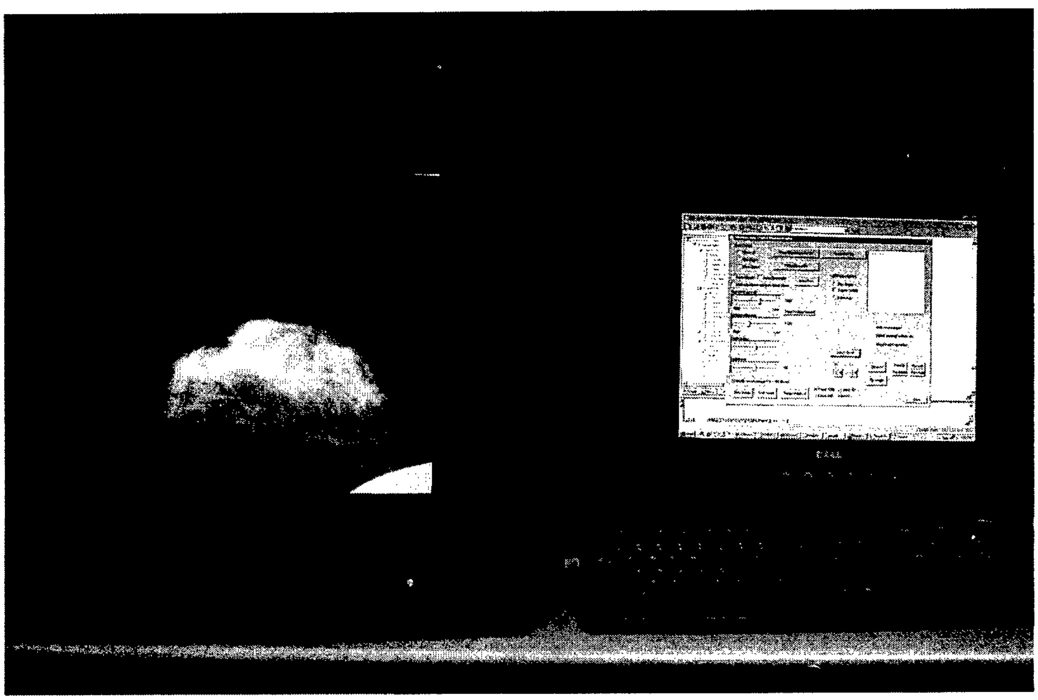

Fig. 2. The DOME-MegaScan PC-based high-resolution stereo display workstation. The first full-field stereomammogram acquired for this project is shown on the monitor.

The DOME Imaging System, Inc, which is a manufacturer of high quality display equipment for medical x-ray images, started to develop a stereo display system when the FFDM became available. They sold us a beta-version, state-of-the-art high-resolution stereo display system at a greatly discounted price. The new display system consists of a DOME Md8-4820-LS stereo graphics board, a MegaScan Md8-4820-LS (8 MegaPixel) 2K stereo monitor, Crystal Eyes stereo glasses, and a Dell OptiPlex 1.8 GHz computer. The DOME-MegaScan system is the only system to-date that can display full-field digital stereomammograms at full resolution (2304 x 1800) and a refresh rate of 120 Hz. It can also display two full-field digital mammograms in non-stereo mode at a refresh rate of 120 Hz. The system is shown in Fig. 2.

Since the DOME Md8-4820-LS stereo graphics board and the stereo display system are not commercial products, the display functions and the user interface are not well developed. We had to develop software to incorporate all of the features of our previous stereo display system including contrast enhancement of 12-bit DICOM images, zooming and panning of the displayed images, and superposition of a virtual cursor on the images for depth measurements. In addition, a graphical user interface (GUI) was incorporated into the display window for the observer performance experiment that compared stereo images and plain images of breast tissue specimens.

(B) Design and Built Stereoscopic Breast Phantoms

We designed two stereoscopic breast phantoms to evaluate the stereomammographic techniques using the GE full field digital mammography system. We had CIRS, Inc. built prototypes of these phantoms. The first one is a rigid breast shape phantom in which 10 groups of simulated microcalcifications and 8 spiculated masses are embedded at different depths. The depths of the center of each group of microcalcifications and masses are provided by the manufacturer. A piece of blue "SMUD" (a PLAYDO-like substance manufactured by Mattel, Inc.) molded into an irregular shape can be placed on top of the phantom to simulate dense tissue. The SMUD produces an under-penetrated area in the x-ray image similar to that in a very dense breast. The second phantom is a compressible breast shape phantom with simulated clustered microcalcifications and masses suspended in a tissue-equivalent gel. The stereomammograms of these phantoms were shown in our previous report.

(C) Evaluation of Depth Measurements using a Stereo Virtual Cursor

In the course of the project, we conceived the idea of using a virtual cursor for measurement of depth in stereomammograms. We evaluated whether the improved depth perception associated with stereomammography might be significantly enhanced with the use of a virtual 3-D cursor. A study was performed to evaluate the accuracy of absolute depth measurements made in stereomammograms with such a cursor [Reportable Outcomes, Journal Articles #1]. The Fischer core biopsy unit was used to produce digital stereo images of a phantom containing 50 low contrast fibrils (0.5-mm diameter nylon monofilaments) at depths ranging from 0 to 10 mm, with a minimum spacing of 2 mm. Half of the fibrils were oriented perpendicular (vertical) and half parallel (horizontal) to the stereo shift direction. The depth and orientation of each fibril were randomized, and the horizontal and vertical fibrils crossed, simulating overlapping structures in a breast image. Left and right eye images were generated by shifting the x-ray tube from $+2.5^{\circ}$ to -2.5° relative to the image receptor. Three observers viewed these images on a computer display with stereo glasses and adjusted the position of a cross-shaped virtual cursor to best match the perceived location of each fibril. The x, y and z positions of the cursor were indicated on the display. The z (depth) coordinate was separately calibrated using known positions of fibrils in the phantom. The observers analyzed images of two configurations of the phantom. Thus, each observer made 50 vertical filament depth measurements and 50 horizontal filament depth measurements. These measurements were compared with the true depths. The correlation coefficients between the measured and true depths of the vertically oriented fibrils for the 3 observers were 0.99, 0.97, and 0.89 with standard errors of the estimates of 0.39 mm, 0.83 mm, and 1.33 mm, respectively. Corresponding values for the horizontally oriented fibrils were 0.91, 0.28, and 0.08, and 1.85 mm, 4.19 mm, and 3.13 mm. All observers could estimate the absolute depths of vertically oriented objects fairly accurately in digital stereomammograms; however, only one observer was able to accurately estimate the depths of horizontally oriented objects. In a subsequent study [Reportable Outcomes, Conference Proceedings #2], we found that most observers' abilities to accurately estimate the depths of horizontally oriented fibrils improved significantly with the use of comb shaped stereo cursors. However, some observers still could not make accurate depth measurements of fibrils in this orientation. This may relate to different aptitudes for stereoscopic visualization.

(D) Effects of Stereo Shift Angle, Geometric Magnification, and Display Zoom on Depth Measurements in Digital Stereomammograms

We performed a study to investigate the effects of stereo shift angle, geometric magnification, and display zoom on the accuracy of depth measurements made with a virtual 3D cursor [Reportable Outcomes, Journal Articles #2]. A phantom containing 50 low contrast fibrils at depths ranging from 1 to 11 mm was imaged with the GE full-field digital mammography system. Left- and right-eye images were generated at stereo shift angles of $\pm3^{\circ}$ and $\pm6^{\circ}$, using either contact or 1.8X geometric magnification geometry. The images were viewed on the high-resolution Barco-Metheus stereoscopic display system in normal and 2X zoom mode. Observers viewed the images with stereo glasses and adjusted the depth of a cross-shaped virtual cursor to best match the perceived depth of each fibril. The results for two trained observers with excellent stereo acuity were nearly identical when viewing the same images. The average root-mean-square errors for the two observers were 1.2 mm ($\pm3^{\circ}$ stereo shift, contact, no zoom), 1.3 mm ($\pm3^{\circ}$ stereo shift, contact, 2X zoom), 0.8 mm ($\pm6^{\circ}$ stereo shift, contact, no zoom), 0.6 mm ($\pm6^{\circ}$ stereo shift, contact, 2X zoom), 0.8 mm ($\pm3^{\circ}$ stereo shift, magnification, no zoom), 0.7 mm ($\pm3^{\circ}$ stereo shift, magnification, 2X zoom), and 0.2 mm ($\pm6^{\circ}$ stereo shift, magnification, no zoom). One observer repeated the entire study for 2 additional fibril phantom configurations. Combining all of the results, we found that for the contact geometry increasing the stereo shift angle from $\pm3^{\circ}$ to $\pm6^{\circ}$ improved the depth measurement accuracy by factors of about 1.2 to 4.0. Zooming did not provide observable improvement in the depth measurement accuracy; sometimes having no effect, sometimes improving the accuracy, and other times reducing the accuracy, with no general trends. The effect of zooming is likely within experimental errors. However, the stereo effect was more readily visualized in the zoom mode. Geometric magnification improved the depth measurement accuracy. The best accuracy among all cases was about 0.2 mm, obtained with geometric magnification using a stereo angle of $\pm6^{\circ}$. This is the mode we recommend for obtaining accurate depth measurements with virtual cursors in stereomammograms.

(E) Effects of Stereoscopic Imaging Technique on Depth Discrimination

Stereoscopic mammography can potentially improve detection of breast cancer by reducing the effects of overlapping tissues and providing 3-dimensional information about a lesion. We evaluated the effects of imaging parameters on depth discrimination of mammographic features [Reportable Outcomes, Conference Proceedings #1]. A breast biopsy unit was used for digital image acquisition. A modular phantom containing 25 pairs of crossing vertical and horizontal fibrils with five different depth separations was designed. The phantom was sandwiched in the middle of 4 cm BR-12 material to simulate the scatter condition for an average breast. Stereoscopic image pairs of three different phantom configurations were acquired at ±2.5° and ±5° stereo-angles and at three different exposure levels with the Fischer Biopsy unit. The images were displayed on the Barco-Metheus Stereo workstation and viewed with LCD stereo glasses. Nine observers visually judged if the vertical fibril in each pair of crossing fibrils was in front of or behind the horizontal fibril. It was found that for viewing fibrils, which simulated spiculations or thin fibrous structures in mammographic images, the accuracy of depth discrimination increased with increasing exposure and stereo-angle in the range studied. However, many observers found it difficult to merge the left-eye and right-eye images to achieve stereovision when the images were acquired with a large stereo-angle.

(F) Effects of Magnification and Zooming on Depth Perception in Digital Stereomammography: An Observer Performance Study

We investigated the effects of magnification and zooming on depth perception [Reportable Outcomes, Conference Proceedings #3 and Journal Articles #3]. A modular phantom was designed which contained six layers of 1-mm-thick Lexan plates, each spaced 1 mm apart. Eight to nine small, thin nylon fibrils were pasted on each plate in horizontal or vertical orientations such that they formed 25 crossing fibril pairs in a projected image. The depth separation between each fibril pair ranged from 2 to 10 mm. A change in the order of the Lexan plates changed the depth separation of the fibril pairs. Stereoscopic image pairs of the phantom were acquired with a GE full-field digital mammography system. Three different phantom configurations were imaged using techniques of 30 kVp, Rh/Rh, ±3° stereo shift angle, contact and 1.8X magnification geometry, and 4 to 63 mAs exposure range. The images were displayed on the Barco-Metheus workstation and viewed with LCD stereo glasses. Five observers participated in the study. Each observer visually judged whether the vertical fibril was in front of or behind the horizontal fibril in each fibril pair. It was found that the accuracy of depth discrimination increased with increasing fibril depth separation and x-ray exposure. The accuracy was not improved by electronic display zooming of the contact stereo images by 2X. Under conditions of high noise (low mAs) and small depth separation between the fibrils, the observers' depth discrimination ability was significantly better in stereo images acquired with geometric magnification than in images acquired with a contact technique and displayed with or without zooming. A 2-mm depth discrimination was achieved with over 60% accuracy on contact images with and without zooming, and with over 90% accuracy on magnification images. This study indicates that stereoscopic imaging, especially with magnification, may be useful for visualizing the spatial distribution of microcalcifications in a cluster and for differentiating overlapping tissues from masses on mammograms.

(G) Collection of Stereoscopic Images of Biopsied Breast Tissue Specimens

We collected a data set of stereoscopic images of breast biopsy tissue specimens for an observer study. A total of 179 samples were imaged in two views with stereo imaging techniques. Therefore, a total of 716 images (179 samples X 2 images per stereo pair X 2 views per sample) were taken with the GE full field digital mammography system. Table I shows the different lesion types in our data set. Of these, images of 21 samples were excluded from the observer study for various reasons. The most frequent problem was that the tissue sample was not shifted properly between the left and right positions during image acquisition so that the two left-eye and right-eye images could not be merged stereoscopically. A few of the samples did not contain the lesion of interest or were too fragmented. Therefore, a total of 158 samples, 63 malignant and 95 benign (Table II), were used in the observer experiment.

Table I. Breast biopsy tissue samples imaged by the stereomammographic technique for the project.

Lesion Type	Mass	Microcalcifications	Mass & Microcalcifications	Total
Malignant	37	25	5	67
Benign	53	52	7	112

Table II. Breast biopsy tissue samples imaged by the stereomammographic technique and used for the observer experiment.

Lesion Type	Mass	Microcalcifications	Mass & Microcalcifications	Total
Malignant	35	23	5	63
Benign	42	47	6	95

(H) ROC Study Comparing Radiologists' Performances in Evaluating Breast Lesions on Stereoscopic and Single-Projection Digital Specimen Mammograms

We are evaluating the effects of stereoscopic imaging on the interpretation of mammographic lesions. In this investigation, we are conducting an observer receiver operating characteristic (ROC) study to compare radiologists' performances in characterizing breast lesions in biopsy tissue specimens from stereo and monoscopic (single-projection) digital mammograms. Stereo and single-projection images of the 158 tissue specimens described above (Table II) were acquired with the GE 2000D digital mammography system in our department. The images are displayed on the DOME-MegaScan stereo display workstation and viewed with LCD glasses. A graphical user interface was developed that allows the user to adjust the image display parameters and to record the Breast Imaging Reporting and Data System (BI-RADS) assessment and confidence ratings on the presence of microcalcifications and masses, margin clearance, and likelihood of malignancy. A preliminary study was conducted with five MQSA radiologists reading the breast lesions in seven sessions. The stereo display mode and the monoscopic display mode of the same specimen were viewed independently in different sessions and in random orders. This minimized the potential memory effects such that the observer would be unlikely to remember the information that he/she had seen on the same specimens displayed in different modes. The observer performances in terms of the area under the ROC curve, A_z, are shown in Table III. For the BI-RADS assessment, the viewing of stereo images resulted in an improvement in the A_z for 4 out of the 7 readings. For the estimation of the likelihood of malignancy, 3 of the 7 readings showed an improvement in the A_z, 2 were reduced, and the other two were comparable. The differences did not reach statistical significance using the Student's paired two-tailed t-test. One of the observers provided a very low A_z (near a chance decision of A_z =0.5) with the stereo images. Although this observer has passed a standard stereo vision acuity test, it appears that the observer may have some difficulty in interpreting clinical image information in stereo images. These equivocal preliminary results may indicate that the radiologists are used to reading mammograms in monoscopic views so that they are unfamiliar with image features in 3D. In order to interpret 3D mammographic features of lesions, the radiologists will need training in reading stereo images.

Table III. Results of a preliminary observer performance experiment that evaluated radiologists' classification of breast lesions in monoscopic (single-projection) and stereoscopic images of biopsied tissue specimens.

	BI-RADS rating		Likelihood of Malignancy rating	
Reading sets	A_z (Mono)	A_z (Stereo)	A_z (Mono)	A_z (Stereo)
1	0.734	0.826	0.759	0.771
2	0.753	0.704	0.756	0.687
3	0.745	0.904	0.754	0.789
4	0.688	0.737	0.717	0.739
5	0.774	0.737	0.778	0.771
6	0.607	0.551	0.619	0.557
7	0.704	0.732	0.725	0.723

In view of the potential difficulty of observers using the stereo image information independently, we have decided to modify the experimental design of the observer experiment. In the new design, the observer will first read the monoscopic view of the image and provide the ratings based on the monoscopic view alone. Immediately after reading the monoscopic image, the observer will be presented with the stereoscopic view. The observer can then change his/her ratings after viewing the stereoscopic image. In this way, the stereoscopic view will provide supplemental information in addition to the monoscopic view for diagnosis of the breast lesions. The combination of monoscopic and stereoscopic viewing will more likely be the method of choice in clinical interpretation because the monoscopic images are readily available in a stereoscopic display and the additional information, if any, should be fully utilized by the radiologists. We will continue the observer performance experiment and present the results in the upcoming AAPM meeting in August, 2003 (Reportable Outcomes, Conference Presentation #11).

(I) Pilot Clinical Study of Stereomammography

We have acquired digital stereomammograms of 7 patients, with IRB approved informed consent, using the stereomammographic imaging technique developed in this project. We showed the first stereomammogram acquired with our technique and displayed on the DOME-MegeScan stereo display workstation in last year's report. As discussed in last year's report, this pilot study was performed as an adjunct to an ongoing pilot clinical trial in the Breast Care Center in the University of Michigan Health System that uses three-dimensional (3D) ultrasound scanning and mammography to monitor the response of breast cancers to neoadjuvant chemotherapy treatment. We plan to investigate if the improved visualization of structures in the stereomammogram, in comparison to a regular mammogram, in combination with 3D ultrasound will improve the identification of tumor response. This does not deviate from the original research plan because the breast cancer patients scheduled for chemotherapy are actually a subset of patients who has suspicious breast lesions. The preliminary results of the pilot study are promising in that the radiologists are impressed with the additional 3D information seen in the stereo images. Since the number of patients is small in this pilot study, we cannot draw conclusions about the significance of the study results. However, this new direction of application of stereomammography will be pursued in continued investigations in the future.

(6) Key Research Accomplishments

- Designed and built a 3D modular phantom for study of depth discrimination with stereoscopic imaging and study of accuracy of depth measurement with 3D virtual cursor -- (Task 1)

- Designed and built stereoscopic 3D breast phantoms with embedded test objects for phantom studies with the full field mammography system -- (Task 1 and Task 5)

- Acquired a high-quality stereo image display from Barco-Metheus. Developed software on a SUN Microsystem workstation for image display, windowing, zooming, panning, and virtual cursors, etc, on the stereo display for performing the observer experiments to optimize the stereoscopic imaging techniques -- (Task 2 and Task 3)

- Acquired a state-of-the-art high-resolution stereo image display workstation from DOME-MegaScan. Developed display functions, virtual cursors, and graphical user interface on a PC for display of full field digital stereomammograms and biopsied breast tissue specimens -- (Task 2, Task 4, Task 5, and Task 6)

- Performed observer experiment to study the effects of stereoscopic imaging techniques on depth discrimination in digital stereomammography -- (Task 3)

- Performed the observer experiment to study the effects of exposure, stereo shift, magnification and display zoom on visual depth discrimination in digital stereomammography -- (Task 3 and Task 5)

- Developed software for generating 3D virtual cursors on stereoscopic display-- (3D virtual cursor and quantitative depth measurement were not in the SOW but are related to Task 3, Task 4, and Task 5)

- Performed observer experiment to study the effects of 3D virtual cursors shape on depth measurements in digital stereomammograms -- (3D virtual cursor and quantitative depth measurement were not in the SOW but are related to Task 3, Task 4, and Task 5)

- Performed observer experiment to study the effects of stereo shift, magnification, and display zoom on the accuracy of depth measurements in digital stereomammograms using 3D virtual cursors -- (3D virtual cursor and quantitative depth measurement were not in the SOW but are related to Task 3, Task 4, and Task 5)

- Developed a stereoscopic image acquisition technique and built a phantom shift device for acquiring stereoscopic image pairs with a clinical full field digital mammography system -- (This technique was not proposed in the SOW but is related to Task 3, Task 4, and Task 5)

- Collected a large database of stereoscopic images of biopsied breast tissue specimens and developed software on DOME-MegaScan stereo display workstation for observer performance study -- (Task 4)

- Performed observer study to evaluate the effects of stereoscopic imaging on the assessment of the likelihood of malignancy and margin clearance of breast lesions using biopsied breast tissue specimens -- (Task 4)

- Collected full field stereomammograms from informed consent patients in a pilot clinical study (Task 6).

(7) Reportable Outcomes

As a result of the support by the BCRP grant, we have conducted extensive studies in stereomammography and published the results. The publications from this research project are listed in the following.

Journal Articles:

1. Goodsitt MM, Chan HP, Hadjiiski LM. Stereomammography: Evaluation of depth perception using a virtual 3D cursor. Medical Physics 2000; 27: 1305-1310.

2. Goodsitt MM, Chan HP, Darner KL, Hadjiiski LM. The effects of stereo shift angle, geometric magnification, and display zoom on depth measurements in digital stereomammography. Medical Physics 2002; 29:2725-2734.

3. Chan HP, Goodsitt MM, Hadjiiski LM, Bailey JE, Klein K, Darner KL, Sahiner B. Effects of Magnification and Zooming on Depth Perception in Digital Stereomammography: An Observer Performance Study. Submitted to Physics in Medicine and Biology.

Conference Proceedings:

1. Chan HP, Goodsitt MM, Darner KL, Sullivan JM, Hadjiiski LM, Petrick N, Sahiner B. Effects of stereoscopic imaging technique on depth discrimination. Presented at the IWDM-2000. Toronto, Canada. June 11-14, 2000. In: Digital Mammography IWDM 2000: 5th International Workshop on Digital Mammography. Ed. Yaffe MJ. (Medical Physics Publishing, Madison, WI) 2001: 13-18.

2. Goodsitt MM, Chan HP, Sullivan JM, Darner KL, Hadjiiski LM. Evaluation of the Effect of Virtual cursor shape on depth measurements in digital stereomammograms. Presented at the IWDM-2000. Toronto, Canada. June 11-14, 2000. In: Digital Mammography IWDM 2000: 5th International Workshop on Digital Mammography. Ed. Yaffe MJ. (Medical Physics Publishing, Madison, WI) 2001: 45-50.

3. Chan HP, Goodsitt MM, Hadjiiski L, Bailey JE, Klein K, Darner KL, Paramagul C. Digital stereomammography: observer performance study of the effects of magnification and zooming on depth perception. Proc SPIE 4682; 2002: 163-166.

Conference Presentation:

1. Goodsitt MM, Chan HP, Hadjiiski LM. Stereomammography: Evaluation of depth perception using a virtual 3-D cursor. Presented at the 85th Scientific Assembly and Annual Meeting of the Radiological Society of North America, Nov. 28-Dec. 3, 1999, Chicago, Illinois. Radiology 1999; 213(P): 368.

2. Chan HP, Goodsitt MM, Darner KL, Sullivan JM, Hadjiiski LM, Petrick N, Sahiner B. Effects of stereoscopic imaging technique on depth discrimination. Presented at The 5th International Workshop on Digital Mammography. IWDM-2000. Toronto, Canada. June 11-14, 2000.

3. Goodsitt MM, Chan HP, Sullivan JM, Darner KL, Hadjiiski LM. Evaluation of the Effect of Virtual cursor shape on depth measurements in digital stereomammograms. Presented at The 5th International Workshop on Digital Mammography. IWDM-2000. Toronto, Canada. June 11-14, 2000.

4. Chan HP, Goodsitt MM., Sullivan JM, Darner KL, Hadjiiski LM. Depth perception in digital stereoscopic mammography. Presented at the Era of Hope Meeting, U. S. Army Medical Research and Materiel Command, Department of Defense, Breast Cancer Research Program, Atlanta, Georgia, June 8-12, 2000.

5. Goodsitt MM, Chan HP, Sullivan JM, Darner KL, Hadjiiski LM. Development of virtual cursors in digital stereomammography. Presented at the Chicago 2000-World Congress on Medical Physics and Biomedical Engineering. Chicago, Illinois, July 23-28, 2000.

6. Goodsitt MM, Chan HP, Hadjiiski LM. The Effect of 2X Zoom on Virtual Cursor Depth Measurements in Stereomammography. Presented at the 43rd Annual Meeting of the American Association of Physicists in Medicine, Salt Lake City, Utah. July 22-26, 2001. Medical Physics 2001; 28, 1247.

7. Chan HP, Goodsitt MM, Hadjiiski LM, Paramagul C, Bailey JE. Digital stereomammography: observer performance study of the effects of magnification and zooming on depth perception. Presented at the SPIE International Symposium on Medical Imaging, San Diego, CA, February, 2002.

8. Chan HP, Goodsitt MM, Hadjiiski LM, Helvie MA, Bailey J, Klein K, Roubidoux MA. Development of digital stereo imaging technique for mammography. Presented at the Era of Hope Meeting, U. S. Army Medical Research and Materiel Command, Department of Defense, Breast Cancer Research Program, Orlando, Florida, September 25-28, 2002.

9. Chan HP, Goodsitt MM, Hadjiiski L, Roubidoux MA, Bailey JE, Helvie MA, Lydick JT, Sahiner B. ROC study comparing radiologists' performances in evaluating breast lesions on stereoscopic and single-projection digital specimen mammograms. Accepted for presentation at the 45th Annual Meeting of the American Association of Physicists in Medicine, San Diego, CA. August 10-14, 2003.

(8) Conclusions

Under the support of this grant, we have acquired two beta high-resolution stereo display workstations and developed software and graphic user interfaces for our research project. We designed and built a modular stereo phantom for evaluation of the effects of stereo imaging techniques on depth discrimination and absolute depth measurement. We also designed a full breast phantom with embedded lesion-mimicking objects and had it built by a phantom manufacturer to evaluate the image quality of stereoscopic imaging.

We conducted a number of observer performance studies to optimize the imaging techniques for acquisition of stereoscopic images. This included the determination of the stereoscopic angle, the magnification factor, the dose requirements, and display zooming. A database of stereo images of biopsied tissue specimens was collected. The database was used in an observer performance experiment in which we compared the accuracies of experienced radiologists in characterizing lesions and in determining margin clearance evaluation from readings of mono and stereo images of the biopsy tissue samples. A pilot study was also performed in which stereomammograms of patients with known breast cancer were acquired and radiologists evaluated the images in comparison with the conventional single-projection mammograms.

In the course of the research, we also developed a new idea of using a 3D virtual cursor for absolute depth measurement for objects in stereo images. A series of observer experiments with phantom images was performed to demonstrate the usefulness and evaluate the accuracy of depth measurement using 3D virtual cursors.

In summary, we performed an extensive investigation of the dependence of the accuracies of depth discrimination and depth measurement on image acquisition techniques in digital stereomammography. Software tools were developed for two high-resolution stereo display workstations The software allows manipulation of the displayed images and provides 3D virtual cursors for the measurement of the depth of a lesion in the image. Observer experiments were performed to evaluate the stereomammography imaging technique using phantoms and biopsied breast tissue samples. A pilot study of comparing full field digital stereomammograms with conventional mammograms was conducted and the image quality of stereomammograms was evaluated by radiologists. Our results indicate that stereomammography is technologically feasible and it is a promising technique that will provide additional 3D information for detection and characterization of breast lesions. Further studies are therefore warranted to investigate whether stereomammography can improve the sensitivity of mammography for breast cancer detection, especially in dense breasts.

(9) Personnel

Name	Role in Project
Heang-Ping Chan, Ph.D.	P.I.
Mitchell M. Goodsitt, Ph.D.	Co-investigator
Mark Helvie, M.D.	Co-investigator
Marilyn A. Roubidoux, M.D.	Co-investigator
Berkman Sahiner, Ph.D.	Co-investigator
Lubomir Hadjiiski, Ph.D.	Co-investigator
Nicholas Petrick, Ph.D.	Co-investigator
Jun Wei, Ph.D.	Postdoc Research Fellow
C. G. Panchal, Ph.D.	Postdoc Research Fellow
Justin Lydick	Student programmer
Jeffrey Sullivan	Student programmer
Chaitanya Gandra	Student programmer
Katie Darner	Research Assistant

(10) Appendix

Copies of the following publications are enclosed with this report. These include all journal articles and proceedings referenced in this report, as well as abstracts that have not been enclosed in previous reports

1. Goodsitt MM, Chan HP, Hadjiiski LM. Stereomammography: Evaluation of depth perception using a virtual 3D cursor. Medical Physics 2000; 27: 1305-1310.

2. Goodsitt MM, Chan HP, Darner KL, Hadjiiski LM. The effects of stereo shift angle, geometric magnification, and display zoom on depth measurements in digital stereomammography. Medical Physics 2002; 29:2725-2734.

3. Chan HP, Goodsitt MM, Hadjiiski LM, Bailey JE, Klein K, Darner KL, Sahiner B. Effects of Magnification and Zooming on Depth Perception in Digital Stereomammography: An Observer Performance Study. Submitted to Physics in Medicine and Biology.

Conference Proceedings:

1. Chan HP, Goodsitt MM, Darner KL, Sullivan JM, Hadjiiski LM, Petrick N, Sahiner B. Effects of stereoscopic imaging technique on depth discrimination. Presented at the IWDM-2000. Toronto, Canada. June 11-14, 2000. In: Digital Mammography IWDM 2000: 5th International Workshop on Digital Mammography. Ed. Yaffe MJ. (Medical Physics Publishing, Madison, WI) 2001: 13-18.

2. Goodsitt MM, Chan HP, Sullivan JM, Darner KL, Hadjiiski LM. Evaluation of the Effect of Virtual cursor shape on depth measurements in digital stereomammograms. Presented at the IWDM-2000. Toronto, Canada. June 11-14, 2000. In: Digital Mammography IWDM 2000: 5th International Workshop on Digital Mammography. Ed. Yaffe MJ. (Medical Physics Publishing, Madison, WI) 2001: 45-50.

3. Chan HP, Goodsitt MM, Hadjiiski L, Bailey JE, Klein K, Darner KL, Paramagul C. Digital stereomammography: observer performance study of the effects of magnification and zooming on depth perception. Proc SPIE 4682; 2002: 163-166.

Conference Abstracts and Presentations:

1. Chan HP, Goodsitt MM, Hadjiiski LM, Helvie MA, Bailey J, Klein K, Roubidoux MA. Development of digital stereo imaging technique for mammography. Presented at the Era of Hope Meeting, U. S. Army Medical Research and Materiel Command, Department of Defense, Breast Cancer Research Program, Orlando, Florida, September 25-28, 2002.

2. Chan HP, Goodsitt MM, Hadjiiski L, Roubidoux MA, Bailey JE, Helvie MA, Lydick JT, Sahiner B. ROC study comparing radiologists' performances in evaluating breast lesions on stereoscopic and single-projection digital specimen mammograms. Accepted for presentation at the 45th Annual Meeting of the American Association of Physicists in Medicine, San Diego, CA. August 10-14, 2003.

The effects of stereo shift angle, geometric magnification and display zoom on depth measurements in digital stereomammography

Mitchell M. Goodsitt,[a] Heang-Ping Chan, Katie L. Darner, and Lubomir M. Hadjiiski
Department of Radiology, University of Michigan, Ann Arbor, Michigan 48109-0030

(Received 23 January 2002; accepted for publication 15 August 2002; published 28 October 2002)

We are developing virtual three-dimensional (3-D) cursors for measuring depths in digital stereomammograms. We performed a study to investigate the effects of stereo shift angle, geometric magnification, and display zoom on the accuracy of depth measurements made with a virtual 3-D cursor. A phantom containing 50 low contrast fibrils at depths ranging from 1 to 11 mm was imaged with a full-field digital mammography system. Left- and right-eye images were generated at stereo shift angles of ±3° and ±6°, using either contact or 1.8× geometric magnification geometry. The images were viewed on a high-resolution stereoscopic display system in normal and 2× zoom mode. Observers viewed the images with stereo glasses and adjusted the depth of a cross-shaped virtual cursor to best match the perceived depth of each fibril. The results for two trained observers with excellent stereo acuity were nearly identical when viewing the same images. The average root mean square errors for the two observers were 1.2 mm (±3° contact, no zoom), 1.3 mm (±3° contact zoom), 0.8 mm (±6° contact, no zoom), 0.6 mm (±6° contact, zoom), 0.8 mm (±3 magnification, no zoom), 0.7 mm (±3° magnification, zoom), and 0.2 mm (±6° magnification, no zoom). One observer repeated the entire study for two additional fibril phantom configurations. Combining all the results, we found that for the contact geometry increasing the stereo shift angle from ±3° to ±6° improved the depth measurement accuracy by factors of about 1.2–4.0. Zooming did not provide observable improvement in the depth measurement accuracy; sometimes having no effect, sometimes improving the accuracy, and other times reducing the accuracy, with no general trends. Its effect is likely within experimental errors. However, the stereo effect was more readily visualized in the zoom mode. Geometric magnification improved the depth measurement accuracy. The best accuracy among all cases was about 0.2 mm, obtained with geometric magnification using a stereo angle of ±6°. This is the mode we recommend for obtaining accurate depth measurements with virtual cursors in stereomammograms. © *2002 American Association of Physicists in Medicine.* [DOI: 10.1118/1.1517615]

Key words: stereomammography, stereoscopic, virtual cursor, 3-D imaging

I. INTRODUCTION

Tissue superposition makes it difficult to accurately interpret conventional mammograms. Such mammograms are acquired using a single projection method whereby (ignoring scatter) the density at a point in the image represents the summation of the attenuation of all tissues along a ray extending from the x-ray tube focal spot to that point. The superpositon of tissues along the rays decreases image contrast and can result in the camouflaging of masses and microcalcifications within dense tissue. It can also lead to superimposed structures having mass-like appearances. The superpositon problem can be reduced or eliminated by generating and viewing 3-D mammograms via multiprojection techniques such as stereoradiography,[1–7] tomosynthesis,[8–10] and computed tomography.[11,12]

We have been investigating digital stereomammography. This is a computerized version of an analog technique that was first described by Warren in 1930.[13] Both the new and old techniques involve taking two separate mammograms, one with the x-ray tube at a positive angle (e.g., +3°) relative to a normal to the detector and the other with the x-ray tube at an equal but opposite angle (e.g., −3°) about the normal. One of the images is viewed with the left eye and the other with the right eye. Our brain fuses the images together to create a 3-D effect. The old technique required taking two films in roughly the same projection. As such, it had several disadvantages, including at least twice the x-ray dose, film cost, and processing time. It also required increased procedure time and radiologist viewing time. Radiologists, in general, eventually decided that these disadvantages outweighed the 3-D visualization advantage, and film stereomammography was discontinued. Digital mammography eliminates or reduces most of these advantages, thereby making digital stereomammography a potentially viable technique. In contrast to screen-film systems, which have sigmoid-shaped response curves, digital detectors have a linear response. Thus, the response curve of the digital detector does not degrade image contrast at lower doses, and it may be possible to utilize half the normal dose for each digital image. The two images of the stereo image pair will be integrated by the observer's eye–brain system to yield about the same signal-to-noise ratio as in a single image taken with the same total dose.[14] With digital systems, image processing and display are almost instantaneous. Also, the method of examining the ences have a 0.6% or smaller effect on the accuracy of the results, which is essentially negligible (e.g., 0.6% of 1.0 mm accuracy=0.006 mm).

When using the tube-shift and phantom-shift methods, it is desirable to align the resulting images such that an object (e.g., a fibril) in contact with the bottom of the phantom does not shift. By doing so, all depths or distances of objects in the phantom will be measured relative to the back surface of the phantom. We achieved the desired zero shift by placing a fiducial marker on the top surface of the slider on which the phantom was placed and digitally translating the resulting left- and right-eye images so that the fiducial markers coincided. For magnification mammography, especially at larger stereo shift angles, the phantom shift method cannot be used because only a portion of the phantom will project to within the field of view of the detector due to the limited size of the detector. For our magnification techniques, we employed the phantom-shift method for the $\pm 3°$ stereo image acquisition and the tube-shift method for the $\pm 6°$ stereo image acquisition. All images in this study were obtained using a technique of 30 kVp, Rh filter, Rh target, 63 mAs. The large (nominal 0.3 mm) focal spot was employed for the contact images and the small (nominal 0.15 mm) focal spot for the (1.8×) geometric magnification images. The scatter-rejection grid was removed for magnification image acquisition.

C. Stereo image display

The stereoscopic display system that was employed for this study consisted of a Barco-Metheus (Beaverton, OR) model 1760S stereo graphics board in a SUN Microsystems (Palo Alto, CA) Ultra 10 computer. The Metheus board operates in a page flipping stereoscopic mode whereby the left- and right-eye images are displayed sequentially, one after the other. This board is capable of displaying 1408×1408×8 bit progressive-scan images at a refresh rate of 114 Hz. The images in our study were displayed on a 21 in. Barco model 521 monitor and viewed with NuVision (Beaverton, OR) LCD stereoscopic glasses. We employed in-house developed software to display, pan, zoom, and adjust the contrast and brightness of the images.

D. Virtual cursor

We developed software to generate the virtual cursors and display their x, y, and z positions. The 3-D nature of the cursor is achieved by introducing offsets in the horizontal positions of the representations of the cursor in the left- and right-eye images. The z coordinate is equal to the offset. When the offset is 0, the cursor is at the same x, y position in both images, and it appears stereoscopically to be at the depth of the monitor screen. As the horizontal offset between the cursor positions is increased in one direction (e.g., left), the cursor appears to move closer to the observer, and as the offset is increased in the opposite direction (e.g., right), the cursor appears to move toward or into the monitor.

E. Z-coordinate calibration

The z coordinate was calibrated by imaging thin wires placed on the steps of a solid acrylic step wedge accurately milled with known step heights. The step wedge was imaged with the GE digital mammography system using the same phantom shift or x-ray tube shift as for the images of the fibril phantoms under the corresponding imaging conditions, and using the fiducial marker alignment technique described previously. The thin wires that were employed for calibration were oriented perpendicular to the tube shift direction. The resulting stereoscopic images were viewed without the stereo glasses and the left- and right-eye cursor positions were adjusted to overlay the left- and right-eye images of the wires on the steps. The z coordinates of the cursor were linearly fit to the known depths of the wires to obtain the calibration line. This calibration was performed for each of the image magnification/zoom conditions discussed below. While this calibration method is accurate and highly reproducible, it relies on the ability of the user to match the positions of the cursors and fibrils in the image and is therefore subjective. A future improvement of the calibration method would entail developing a computer program to determine the positions of the fibrils (e.g., their centers of masses).

F. True fibril depths

Through a careful examination of the fibril phantom, we noticed that minor warping of the sandwiched Lexan plates could cause the actual depths of the fibrils to differ from their nominal 1, 3, 5, 7, 9, and 11 mm values. To more accurately determine the true depths of the fibrils for each phantom layer configuration, we applied the calibration method described above to one set of the stereo pair images. The $\pm 6°$ magnification image pair was selected because the displacements in the fibril locations between the left- and right-eye images are the greatest for this image pair. The larger displacement results in greater localization accuracy since the limitation of approximately ± 1 pixel uncertainty in placement of the stereo cursors on the fibrils in the images will correspond to a smaller uncertainty in the actual depth. A third observer who was different from the two who participated in the observer study described below viewed, without the stereo glasses, the $\pm 6°$ magnification stereo pair images of the phantoms in the three multilayer configurations studied and adjusted the left- and right-eye cursor components to overlay each fibril. The measured z values were then converted to true depths in millimeters using the calibration lines derived with the step wedge phantom. In performing this procedure, we found that when the nominal 1 mm depth fibrils (i.e., those that were a distance of 1 mm from the bottom of the phantom) were viewed without the glasses, they were too close to each other for the accurate positioning of overlaying cursors. We therefore could not determine their true depths and only analyzed the true depths of the fibrils at the nominal 3, 5, 7, 9, and 11 mm depths in the phantoms. Hence, the results in this paper are only presented at those depths. This is a consequence of the method that was employed to determine the true depths and would not be a limi-

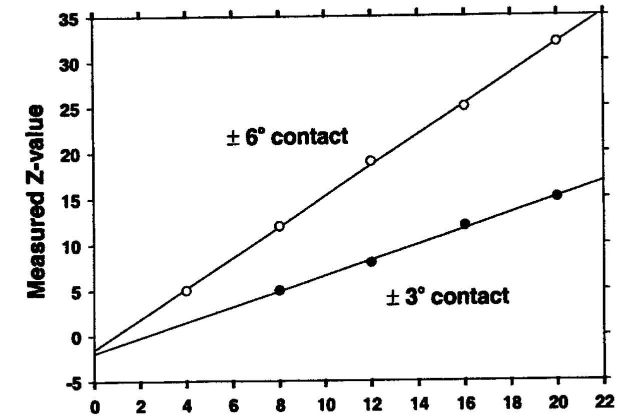

(a)

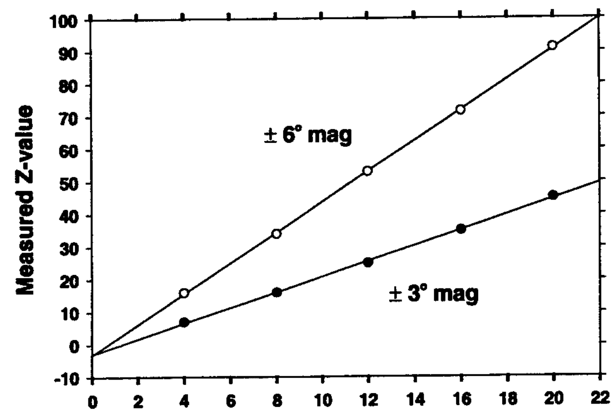

(b)

FIG. 3. (a) Calibration lines for ±3° stereo shift contact and ±6° stereo shift contact acquisition; (b) calibration lines for ±3° stereo shift magnification and ±6° stereo shift magnification acquisition.

ometry are compared in part (b). For the 2×-zoom mode, our cursor software effectively incremented the z values in steps of 0.5 per pixel shift instead of steps of 1 for the nonzoom mode. Consequently, the calibration lines that were computed in the 2×-zoom display modes were nearly identical to those in the nonzoom modes and they are therefore not shown in the figures. The calibration equations for the conversion of the measured z values to the depths (distances from the back of the phantoms) for the various imaging conditions are listed in Table I, below.

TABLE I. Calibration equations for converting measured z values to depths (distances in front of the backside of the phantom). *Note:* these calibration equations were derived by linearly fitting the data acquired from the step wedge images. Examples of the lines for the step wedge data are shown in Fig. 1.

Stereo Shift Angle	Geometry	Display zoom	Equation
±3 degrees	Contact	None	Depth (mm) $=\frac{Z+1.9}{0.85}$
±3 degrees	Contact	2×	Depth (mm) $=\frac{Z+1.55}{0.825}$
±6 degrees	Contact	None	Depth (mm) $=\frac{Z+1.5}{1.675}$
±6 degrees	Contact	2×	Depty (mm) $=\frac{Z+2.5}{1.75}$
±3 degrees	Magnification	None	Depth (mm) $=\frac{Z+2.9}{2.375}$
±3 degrees	Magnification	2×	Depth (mm) $=\frac{Z+2.6}{2.35}$
±6 degrees	Magnification	None	Depth (mm) $=\frac{Z+3.15}{4.688}$

Results comparing the performances of the two observers for the various stereo angle, geometric magnification, and display zoom combinations of the experiment are summarized in Tables II–IV. Examples of plots of the measured versus true depths for one observer for each of the imaging conditions are shown in Fig. 4. Errors in the depth measurements for each imaging condition for the one observer who viewed images in two additional phantom configurations are listed in Table IV. The paired t-test results for the observer who measured the z values of the fibrils in the phantom in three separate phantom layer configurations are listed in Table V. (Note, the paired t-test results for the other observer who made measurements of the fibrils in the first phantom configuration were very similar to those listed in part A of this table and are therefore not shown.)

The reproducibility of the observer's measurements in the same image read twice was excellent. For the 40 fibrils that were analyzed in the image, 35 of the measured z values were the same for both readings, and the remaining 5 z values differed by ±1. This translates to a rms difference in the z values of 0.354 (i.e., $\sqrt{5/40}$), which is equal to 0.21 mm.

TABLE II. Linear fit parameters for measured versus true depths of fibrils for two observers (values for observer 1 are indicated by subscript 1, and for observer 2 by subscript 2).

	3°	3° zoom	6°	6° zoom	3° mag	3° mag zoom	6° mag
r_1	0.956	0.949	0.994	0.996	0.982	0.978	0.998
r_2	0.934	0.921	0.994	0.996	0.985	0.981	0.998
intercept_1	0.669	0.030	−0.757	−0.306	−0.822	−0.470	−0.013
intercept_2	1.379	0.930	−0.910	−0.502	−0.777	−0.476	−0.082
slope_1	0.969	1.041	1.000	0.978	1.031	1.007	0.994
slope_2	0.961	1.002	1.037	0.997	1.049	1.016	1.004
SEE_1	0.884	1.036	0.331	0.263	0.604	0.656	0.170
SEE_3	1.103	1.264	0.329	0.254	0.560	0.606	0.174

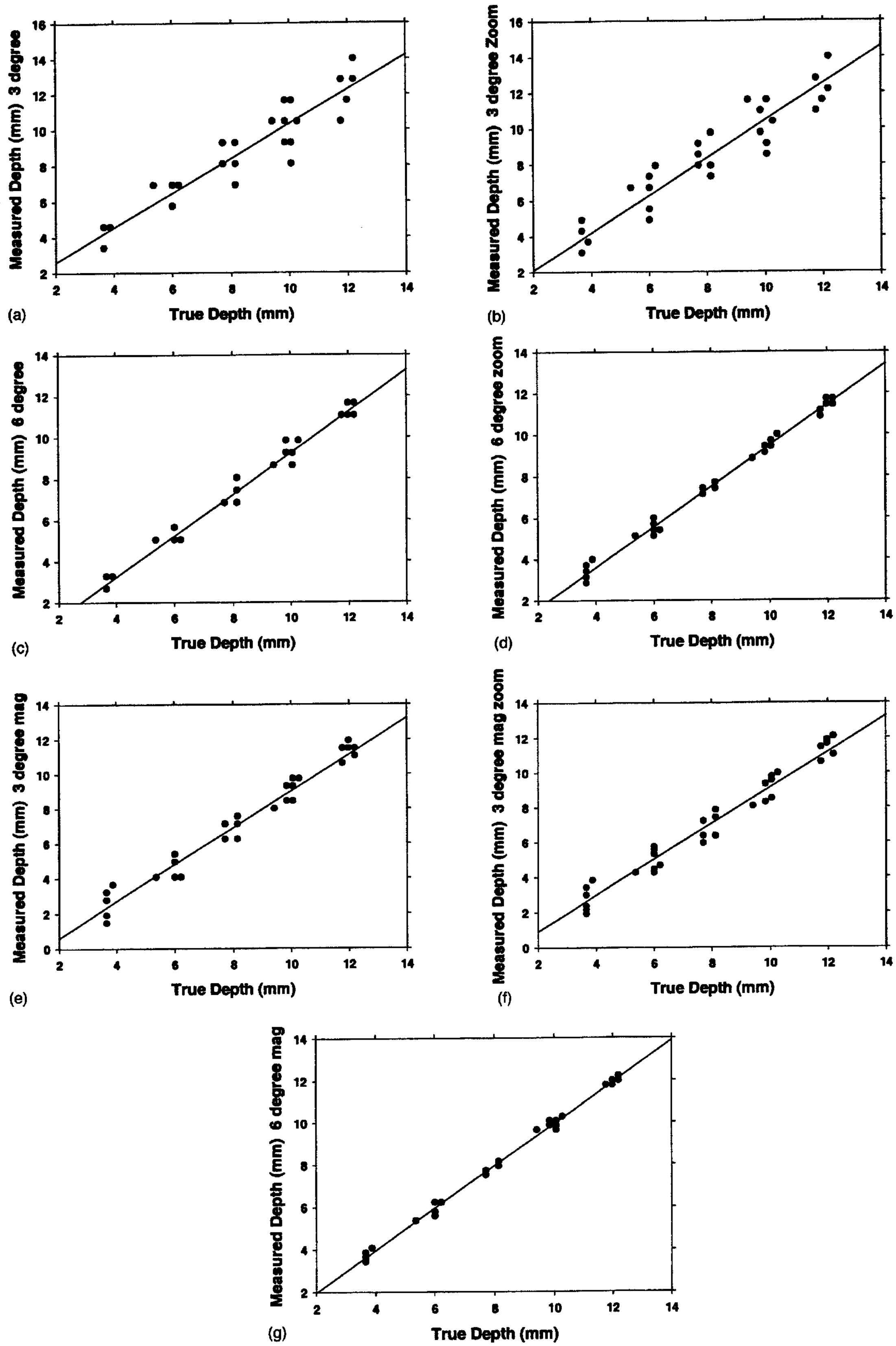

FIG. 4. Examples of measured versus true depths (distances from the back of the phantom) for observer number 1. (a) Stereo shift angle $=\pm 3°$, contact, no zoom; (b) stereo shift angle $=\pm 3°$, contact, zoom=2; (c) stereo shift angle $=\pm 6°$, contact, no zoom; (d) stereo shift angle $=\pm 6°$, contact, zoom=2; (e) stereo shift angle $=\pm 3°$, magnification mode, no zoom; (f) stereo shift angle $=\pm 3°$, magnification mode, zoom=2; (g) stereo shift angle $=\pm 6°$, magnification mode, no zoom.

fore likely caused by experimental uncertainties due to the many factors described above. Thus, artificially increasing the displacement between objects viewed in the left- and right-eye stereo pairs through zooming the display does not have the same effect as increasing the displacement via increasing the stereo shift angle or increasing the geometric magnification. The stereo effect was more readily visualized in the zoom mode, but the signal-to-noise ratios of the fibril images were basically the same as those in the images displayed without zoom. In contrast, the acquisition of images with geometric magnification actually improves the signal-to-noise ratio.[18] The 2× zoom that was employed in this study was achieved by pixel replication. Results may be different for interpolative zoom. Finally, the use of greater zoom factors was also not explored. However, based on the results of a recently published study, increasing the display zoom factor may not be beneficial.[19] In that study, the observers' stereoacuities and depth perceptions were compared using a standard Randot stereotest pattern, with and without magnification via a 4× optical loupe and a 16× microscope. The researchers found that stereo acuity and depth perception decreased with increasing optical magnification of the pattern.

The paired *t*-test results listed in Table V indicate the majority of the differences between the depth measurement accuracies obtained with the ±3° and ±6° stereo shift angles, magnification and contact geometries, and normal and zoom displays are statistically significant ($p<0.05$). It is interesting to note that there was little consistency between the categories of the small number of insignificant differences ($p>0.05$) for the images created with the three different phantom configurations (parts A, B, and C of Table V). The only consistent insignificant result was that in two of the three cases, the accuracies for the ±3° mag and ±3° mag zoom depth measurements were not statistically significant. The *t*-test results for the two observers were quite similar for phantom configuration #1 (see footnote "a" of Table V, part A). Increasing the number of observers would have increased the statistical power of this study; however, the variability in the results due to the various factors described above would not have been reduced. Therefore the conclusions would likely be the same.

The best accuracy of about 0.2 mm, among all cases, was obtained with geometric magnification using a stereo angle of ±6°. Therefore, this is the mode we recommend for obtaining accurate depth measurements with virtual cursors in stereomammograms. Conventional stereoradiography is performed in contact mode using a stereo shift angle of ±3°. According to Christensen,[20] this angle was determined empirically "by trial and error." The angle is a compromise between the improved stereoscopic effect with increasing angle, the increased eye strain and difficulty in fusing the left- and right-eye images, especially at larger stereo angles, and the reduced patient coverage at larger stereo angles. For our particular case, the increased stereoscopic effect associated with the use of twice the conventional stereo angle and the use of ~1.8× geometric magnification did not cause undue eye strain. It did reduce the imaged field of view and this geometry could not be used for imaging an entire breast unless a larger-area detector was employed. Based on our measurements and observations, we recommend for stereoscopic imaging and depth measurements within an entire breast with the GE full-field digital mammography system, that a contact geometry be employed using a stereoshift angle of ±6° instead of the conventional ±3°. The overall results and recommendations of this study may differ for detectors having different pixel sizes and noise properties and for displays with different noise and contrast. A further investigation of the effects of these factors is warranted.

Finally, the depth measurement accuracies of the two observers in this study (Table III) were almost identical (in nearly all cases they were within 0.1 mm of each other). Both observers had excellent stereo acuity, and it would be expected that others with similar stereo acuity could achieve similar results after a period of training. Our previous studies with other observers have shown that there is a wide range of accuracies for depth measurements, especially for horizontally oriented objects.[3] All of the fibrils in this study had horizontal and vertical components, so it would be expected that even observers who have difficulties measuring the depths of horizontally oriented objects would be able to measure the depths of the diagonally oriented fibrils, although their accuracies may not be as high. Since it is unlikely that fibrous tissues or spicules from masses in mammograms are exactly horizontal to the stereo shift direction, the angulation would enable reasonably accurate measurements in clinical images. However, the inhomogeneous anatomical background within the clinical images may partially obscure the fibrils, which would increase the difficulty of making accurate depth measurements with the stereo cursor. It is possible that with additional training and the use of depth cues (e.g., 3-D wire boxes placed about the objects of interest, or 3-D rulers in the image) in clinical images, the depth measurement accuracies of most viewers would be adequate. The development of such depth cues will be the subject of our future investigations.

ACKNOWLEDGMENTS

This work is supported by U.S. Army Medical Research and Material Command Grants No. DAMD 17-98-1-8210 and No. DAMD 17-99-1-9294. The content of this publication does not necessarily reflect the position of the funding agency, and no official endorsement of any equipment and product of any companies mentioned in this publication should be inferred.

[a]Corresponding author: Department of Radiology, University of Michigan Hospitals, Room B1 F510C, 1500 East Medical Center Drive, Ann Arbor, Michigan 48109-0030. Office 734-936-7474; Fax: 734-936-7948; Electronic mail: goodsitt@umich.edu

[1]D. M. Chelberg, J. Hsu, C. G. Babbs, Z. Pizlo, and E. J. Delp, "Digital stereomammography," in *Proceedings of the 2nd International Workshop on Digital Mammography*, Excepta Medica International Congress Series 1069 (Elsevier Science, York, England, 1994), pp. 181–190.

[2]J. Hsu, D. M. Chelberg, C. F. Babbs, Z. Pizlo, and E. J. Delp, "Preclinical ROC studies of digital stereomammography," IEEE Trans. Med. Imaging **14**, 318–327 (1995).

Stereomammography: Evaluation of depth perception using a virtual 3D cursor

Mitchell M. Goodsitt,[a] Heang-Ping Chan, and Lubomir Hadjiiski
Department of Radiology, University of Michigan, Ann Arbor, Michigan 48109-0030

(Received 22 October 1999; accepted for publication 28 March 2000)

We are evaluating the usefulness of stereomammography in improving breast cancer diagnosis. One area that we are investigating is whether the improved depth perception associated with stereomammography might be significantly enhanced with the use of a virtual 3D cursor. A study was performed to evaluate the accuracy of absolute depth measurements made in stereomammograms with such a cursor. A biopsy unit was used to produce digital stereo images of a phantom containing 50 low contrast fibrils (0.5 mm diam monofilaments) at depths ranging from 1 to 11 mm, with a minimum spacing of 2 mm. Half of the fibrils were oriented perpendicular (vertical) and half parallel (horizontal) to the stereo shift direction. The depth and orientation of each fibril were randomized, and the horizontal and vertical fibrils crossed, simulating overlapping structures in a breast image. Left and right eye images were generated by shifting the x-ray tube from $+2.5°$ to $-2.5°$ relative to the image receptor. Three observers viewed these images on a computer display with stereo glasses and adjusted the position of a cross-shaped virtual cursor to best match the perceived location of each fibril. The x, y, and z positions of the cursor were indicated on the display. The z (depth) coordinate was separately calibrated using known positions of fibrils in the phantom. The observers analyzed images of two configurations of the phantom. Thus, each observer made 50 vertical filament depth measurements and 50 horizontal filament depth measurements. These measurements were compared with the true depths. The correlation coefficients between the measured and true depths of the vertically oriented fibrils for the three observers were 0.99, 0.97, and 0.89 with standard errors of the estimates of 0.39 mm, 0.83 mm, and 1.33 mm, respectively. Corresponding values for the horizontally oriented fibrils were 0.91, 0.28, and 0.08, and 1.87 mm, 4.19 mm, and 3.13 mm. All observers could estimate the absolute depths of vertically oriented objects fairly accurately in digital stereomammograms; however, only one observer was able to accurately estimate the depths of horizontally oriented objects. This may relate to different aptitudes for stereoscopic visualization. The orientations of most objects in actual mammograms are combinations of horizontal and vertical. Further studies are planned to evaluate absolute depth measurements of fibrils oriented at various intermediate angles and of objects of different shapes. The effects of the shape and contrast of the virtual cursor and the stereo shift angle on the accuracy of the depth measurements will also be investigated. © *2000 American Association of Physicists in Medicine.* [S0094-2405(00)01406-1]

Key words: stereomammography, stereoscopic, virtual cursor, three-dimensional

I. INTRODUCTION

Presently, screening x-ray mammography is the only technique that has a proven capability for detecting early stage clinically occult cancers.[1] Although mammography has a high sensitivity for detecting breast cancers, studies have shown that radiologists do not detect all carcinomas that are visible on retrospective analyses of the mammograms.[2–11] These missed detections are often a result of the very subtle nature of the mammographic findings. One of the major deficiencies of mammography is the inability to discern masses and microcalcifications hidden in dense fibroglandular tissue.[12] It is estimated that about 20% of the breast cancers in dense breasts are not detected by mammography.[9,11] Conventional mammography is a two-dimensional projection image of a three-dimensional structure. As a result, objects along the same x-ray beam path overlap each other. The overlying tissue structures often obscure the visibility of subtle lesions of interest in the mammogram. The camouflaging of the anatomical structures is the main cause of missed diagnoses. Overlapping structures can also project onto the image plane forming shadows that appear to be lesions, resulting in false positive findings. Radiologists examine two or more projections of each breast to improve their ability to detect lesions and to assist them in distinguishing between true lesions and overlapping tissues. However, standard mammographic techniques are not always successful in distinguishing true lesions from overlapping tissues. Digital stereomammography is a method that could potentially solve many of these problems.

Stereomammography is not a new technique. It was first described in 1930.[13] Like other forms of stereoradiography at that time, it involved taking two film images, a left eye image and a right eye image. These were obtained by positioning the x-ray tube at a certain distance to the left and to the

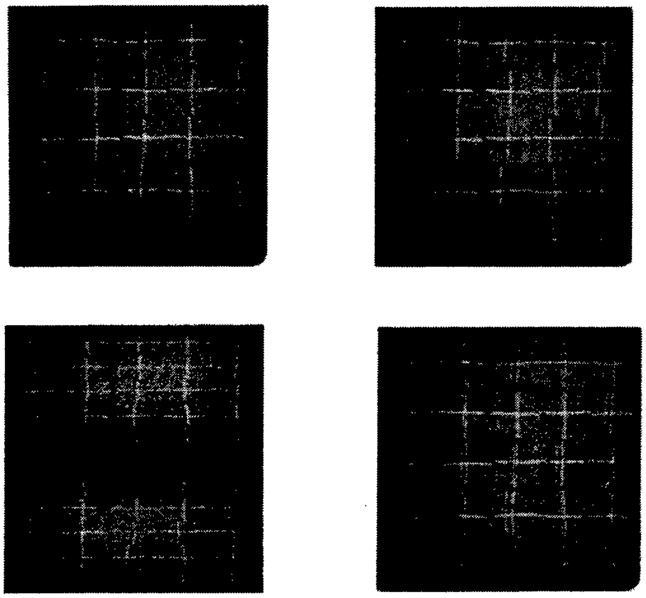

FIG. 2. (Top) Left and right eye images of the phantom shown in Fig. 1. The image pair was obtained with a stereoscopic angle of ±2.5° about the central axis. The fibril pairs with the smallest spacing of 2 mm in this phantom can be identified and the relative depths of the different fibrils can also be clearly distinguished. (Bottom left) Image of the phantom that is stored in the computer frame buffer. This image is synch-doubled by the display processor for stereoscopic viewing. Synch-doubling enables viewing of the left- and right-eye images at twice the nominal refresh rate of the display monitor for reduced flicker. The left-eye image is stored in the frame buffer at the top, and the right-eye image at the bottom. An additional vertical synch pulse is inserted between the two images to produce the two separate images shown at the top of this figure. (Bottom right) Image formed by combining the left- and right-eye images into one. An image similar to this is seen when one views the display without the stereoscopic glasses, and is the one used to calibrate the virtual cursor. The virtual cursor (not shown above) appears as two cursors (a left-eye cursor and a right-eye cursor) when the images are viewed without the stereo glasses, and the horizontal separation between the cursors changes as the cursor depth is adjusted.

Physics of Diagnostic Radiology,[14] early radiologists learned by "trial and error that a tube shift equal to 10% of the target-film distance produced satisfactory results."[14] This tube shift is equal to a total stereo-shift angle of about 6° (e.g., +3° and −3° relative to a line perpendicular to the image receptor.) In general, larger tube shifts produce improved depth perception, but beyond a certain limit, this is achieved at the expense of increased observer fatigue[26] and decreased stereo field of view. The angle scale on the Fischer unit is marked in 5° increments, and our preliminary investigations with the Fischer digital system indicated a stereo shift of +2.5° to −2.5° produced images that appeared to have adequate depth discrimination without producing undue eyestrain. This stereo angle was therefore used for image acquisition in this study. It corresponds with a total stereo shift of about 9% (5.94 cm) for the 68 cm source-to-image distance of the Fischer system. Future studies will be performed to determine the optimal angle for accurate depth perception with acceptable eyestrain. The Fischer unit has a fiber optic-coupled CCD detector that produces 1024×1024 ×12-bit images. The images can be stored in 1024×1024 ×8-bit TIFF format or transmitted to a DICOM server. We

TABLE I. Linear regression results for measured vs true depths in phantom images. (A) Vertically oriented fibrils. (B) Horizontally oriented fibrils.

Reader	Image	Slope	Intercept	r-value	SEE (mm)
(A)					
A	1	1.025	−0.56	0.992	0.39
A	2	1.017	−0.56	0.994	0.38
Average *A*				0.993	0.39
B	1	0.845	−0.65	0.887	1.33
B	2	0.868	−0.61	0.891	1.32
Average *B*				0.889	1.33
C	1	1.087	−1.62	0.963	0.92
C	2	0.955	0.00	0.968	0.74
Average *C*				0.966	0.83
Overall average		0.966	−0.67	0.949	0.85
(B)					
A	1	1.129	−3.04	0.947	1.24
A	2	1.135	−4.66	0.871	2.50
Average *A*				0.909	1.87
B	1	0.003	−5.57	0.004	2.55
B	2	0.176	−7.52	0.154	3.71
Average *B*				0.079	3.13
C	1	0.189	−3.70	0.135	4.54
C	2	0.558	−4.96	0.431	3.83
Average *C*				0.283	4.19
Overall average		0.532	−4.91	0.424	3.06

employed the TIFF formatted images in this study. Since no contrast enhancement was performed on the displayed images in the observer study, it is unlikely that a bit depth greater than 8 bits could have been perceived in the displayed images. Therefore, it is unlikely that compression to 8 bits influenced our results.

C. Stereoscopic viewer and virtual cursor

The images were displayed on a personal computer using a Model SS-03 Stereo Display Processor from Neotek, Inc. (Pittsburgh, PA). We used Neotek's Composer software to format the images and their optional Presenter software to display the images along with a virtual cursor. The Presenter software also generates a display of the x, y, and z-positions of the virtual cursor. The Neotek system produces stereo images via a method termed "synch-doubling." In this method, the left eye image is stored above the right eye image in the video graphics board (see Fig. 2), and an additional vertical synch pulse is inserted between the two images in the video signal coming from the computer. This synch-doubling causes the images to be displayed fully on the monitor at twice the normal refresh rate for reduced flicker (i.e., if the board is run at a 60 Hz refresh rate, the images are displayed at 120 Hz). The graphics board was operated in the 1024 (horizontal)×768 (vertical) resolution mode recommended by Neotek. The Neotek Composer software downsized the 1024×1024 images to fit two images (the left on top of the right) within this resolution. That is, it converted the left and right eye images to each be about

TABLE II. Root mean square (RMS) errors of measured depths of fibrils.[a] (A) Vertically oriented fibrils. (B) Horizontally oriented fibrils.

Reader	Image	RMS error (mm)
(A)		
A	1	0.59
A	2	0.62
B	1	1.91
B	2	1.78
C	1	1.53
C	2	0.75
Overall average		1.20
(B)		
A	1	2.70
A	2	4.76
B	1	11.36
B	2	12.56
C	1	9.30
C	2	8.24
Overall Average		8.15

[a]RMS error $=\sqrt{\Sigma_{i=1}^{25}(\text{true depth}_i-\text{measured depth}_i)^2/25}$.

rate to within 2 mm. This is consistent with relative stereoscopic studies performed by Doi and Duda[26] and Higashida *et al.*[15] and absolute stereoscopic studies performed by Fencil *et al.*[16] Doi and Duda and Higashida *et al.* investigated observers' abilities to distinguish (as opposed to measure) the separation of objects that were superimposed on stepwedge phantoms. In Doi and Duda's study,[26] the objects were 0.2 mm diam aluminum wires. A matrix of "plus" objects were formed by placing horizontally and vertically oriented pieces of wire at the bottom of the stepwedge, with their counterparts located directly above on the step of known thickness (e.g., horizontal wire on step if bottom wire is vertical). The "plus" objects were imaged stereoscopically using a geometric magnification factor of 2 and x-ray focal spot shifts of 1.25%, 2.5%, and 5% of the focus-to-film distance. These investigators found that observers could correctly identify 1 mm separations between two aluminum wires 80% of the time for the 5% tube shift and between 60 and 70% for the other tube shifts. In Hagashida *et al.*'s study,[15] a similar phantom was used. Teflon tube objects filled with contrast media were arranged on the stepwedge to form cross (or "X") shaped objects. They employed a geometric magnification factor of 1.1 and the x-ray focal spot shift for stereoscopic imaging was 6.5% of the focus-to-image intensifier distance. They found that observers could correctly identify 1.6 mm separations between 1 mm diameter tubes containing 25% iodine contrast more than 80% of the time.

Our study and results can be distinguished from those of Doi and Duda[26] and Higashida *et al.*[15] because we investigated absolute rather than relative stereoscopic measurements and because we analyzed horizontally and vertically oriented objects separately. With respect to absolute measurements, Fencil *et al.*[16] imaged a box phantom containing aluminum wires that simulated blood vessels at different angles. Fencil *et al.* employed an automated cross-correlation technique to determine the position of a wire (vessel) segment in the second image of a stereoscopic pair after it was selected in the first image. They obtained an average calculated distance error of approximately ± 2 mm, which is similar to our error for vertically oriented fibrils and the errors in the studies of Doi and Duda and Higashida *et al.* that are cited above. Our technique is easier to implement than Fencil *et al.*'s but more observer dependent, as the observer effectively judges the correlation between the cursor and the fibrils in both images of the stereoscopic pair.

The fact that the observers in our study did worse at measuring the depths of horizontally as opposed to vertically oriented fibrils is not surprising since the image discrepancy and hence the stereoscopic effect is less for the horizontal objects (i.e., there is considerable overlap between corresponding horizontally oriented objects in the stereo pairs, and the shifts in positions are not as apparent).[14] There appears to be a larger difference in the performance among the observers for the horizontally oriented fibrils, with one observer performing very well and the other two very poorly. This may be related to different aptitudes for stereoscopic visualization.

The orientations of most objects in actual mammograms are combinations of horizontal and vertical. Further studies are planned to evaluate absolute depth measurements of fibrils oriented at various intermediate angles and of objects of different shapes. The effects of the shape and contrast of the virtual cursor and of the stereo shift angle on the accuracy of the depth measurements will also be investigated. Finally, the cursors will be applied to digital stereomammograms of breast biopsy samples to determine their applicability in estimating lesion depths and dimensions and in providing additional depth cues for improved stereoscopic image interpretation.

ACKNOWLEDGMENTS

This work is supported by U.S. Army Medical Research and Materiel Command Grant DAMD 17-98-1-8210. The content of this publication does not necessarily reflect the position of the funding agency, and no official endorsement of any equipment and product of any companies mentioned in this publication should be inferred.

[a)]Send all correspondences to the following address: Department of Radiology, University of Michigan Hospitals, Room B1 F510C, 1500 East Medical Center Drive, Ann Arbor, Michigan 48109-0030. Office: 734-936-7474; Fax: 734-936-7948; electronic mail: goodsitt@umich.edu

[1]H. Seidman, S. K. Gelb, E. Silverberg, N. LaVerda, and J. A. Lubera, "Survival experience in the Breast Cancer Detection Demonstration Project," CA-Cancer J. Clin. **37**, 258–290 (1987).

[2]M. Moskowitz, *Benefit and Risk*, in *Breast Cancer Detection: Mammography and Other Methods in Breast Imaging*, 2nd ed., edited by L. W. Bassett and R. H. Gold (Grune and Stratton, New York, 1987).

[3]J. E. Martin, M. Moskowitz, and J. R. Milbrath, "Breast cancer missed by mammography," AJR, Am. J. Roentgenol. **132**, 737–739 (1979).

[4]B. J. Hillman *et al.*, "Mammogram interpretation by physician assistants," AJR, Am. J. Roentgenol. **149**, 907–911 (1987).

[5]L. Kalisher, "Factors influencing false negative rates in xeromammography," Radiology **133**, 297–301 (1979).

Effects of Magnification and Zooming on Depth Perception in Digital Stereomammography: An Observer Performance Study

Heang-Ping Chan

Mitchell M. Goodsitt

Lubomir M. Hadjiiski

Janet E. Bailey

Katherine Klein,

Katie L. Darner

Berkman Sahiner

Department of Radiology

University of Michigan, Ann Arbor, MI 48109

Short Title: Depth Perception in Digital Stereomammography

Correspondence:

Heang-Ping Chan, Ph.D.
Department of Radiology
University of Michigan
1500 E. Medical Center Dr.
UH B1F510B
Ann Arbor, MI 48109-0030
phone: 734-936-4357
fax: 734-615-5513
email: chanhp@umich.edu

ABSTRACT

We are evaluating the application of stereoscopic imaging to digital mammography. In the current study, we investigated the effects of magnification and zooming on depth perception. A modular phantom was designed which contained six layers of 1-mm-thick Lexan plates, each spaced 1 mm apart. Eight to nine small, thin nylon fibrils were pasted on each plate in horizontal or vertical orientations such that they formed 25 crossing fibril pairs in a projected image. The depth separation between each fibril pair ranged from 2 to 10 mm. A change in the order of the Lexan plates changed the depth separation of the two fibrils in a pair. Stereoscopic image pairs of the phantom were acquired with a GE full-field digital mammography system. Three different phantom configurations were imaged. All images were obtained using a Rh target/Rh filter spectrum at 30 kVp tube potential and a ±3° stereo shift angle. Images were acquired in both contact and 1.8X magnification geometry and an exposure range of 4 to 63 mAs was employed. The images were displayed on a Barco monitor driven by a Metheus stereo graphics board and viewed with LCD stereo glasses. Five observers participated in the study. Each observer visually judged whether the vertical fibril was in front of or behind the horizontal fibril in each fibril pair. It was found that the accuracy of depth discrimination increased with increasing fibril depth separation and x-ray exposure. The accuracy was not improved by electronic display zooming of the contact stereo images by 2X. Under conditions of high noise (low mAs) and small depth separation between the fibrils, the observers' depth discrimination ability was significantly better in stereo images acquired with geometric magnification than in images acquired with a contact technique and displayed with or without zooming. Under our experimental conditions, a 2-mm depth discrimination was achieved with over 60% accuracy on contact images with and without zooming, and with over 90% accuracy on magnification images. This study indicates that stereoscopic imaging, especially with magnification, may be useful for visualizing the spatial distribution of microcalcifications in a cluster and for differentiating overlapping tissues from masses on mammograms.

KEY WORDS: Digital mammography, stereoscopic imaging, magnification, zooming, observer performance study.

1. INTRODUCTION

At present, x-ray mammography is the only diagnostic procedure with a proven capability for detecting early stage, clinically occult breast cancers (Seidman *et al*, 1987). Although mammography has a high sensitivity for detection of breast cancers when compared to other diagnostic modalities, studies indicate that radiologists do not detect all carcinomas that are visible on retrospective analyses of the images (Wallis *et al*, 1991; Bird *et al*, 1992; Harvey *et al*, 1993; Beam *et al*, 1996). These missed detections are often a result of the very subtle nature of the radiographic findings. However, one of the major deficiencies of mammography is its inability to discern lesions hidden behind dense fibroglandular tissues (Jackson *et al*, 1993). It is estimated that about 20% of the breast cancers in dense breasts are not detected by mammography (Wallis *et al*, 1991; Bird *et al*, 1992). It is therefore important to improve the sensitivity of mammography in imaging dense breasts. With the advent of high resolution digital detectors, new breast imaging techniques such as stereomammography (Goodsitt *et al*, 2000; Chan *et al*, 2001; Getty *et al*, 2001; Goodsitt *et al*, 2002; Maidment *et al*, 2003), digital tomosynthesis (Niklason *et al*, 1997; Suryanarayanan *et al*, 2000), and computed tomography (Raptopoulos *et al*, 1996; Boone *et al*, 2001) are being developed to alleviate this problem.

A conventional radiograph is a projection image. The anatomical structures along the x-ray beam path are projected onto a two-dimensional image plane and overlap with each other. The overlying tissue structures often obscure the visibility of subtle lesions of interest in a radiograph. The camouflaging effect of the anatomical structures is the main cause of missed diagnosis. Stereoscopic imaging will allow the overlying structures to be perceived at different depths, thereby reducing the camouflaging effect. It has been reported that digital stereomammography allowed the detection of additional lesions that were obscured on screen-film mammograms (Getty *et al*, 2001).

Stereoscopic radiography has been attempted for different types of examinations (Doi *et al*, 1981; Kelsey *et al*, 1982; Doi and Duda, 1983; Higashida *et al*, 1988; Trocme *et al*, 1990; Ragnarsson and Karrholm, 1992). The principle of stereoscopic imaging is shown in Fig. 1. The x-ray focal spot is shifted, along a direction parallel to the image plane, to the left and the right of the central axis to obtain two images of the object. The object has to remain stationary during the process. The images are referred to as the left-eye (LE) and the right-eye (RE) image. When the two images are positioned properly and viewed by trained eyes or with the aid of a stereoscope so that the left eye sees only the LE image and the right eye sees only the RE image, the parallax between the two images creates the depth perception. It is important to match the amount of stereoscopic shift to the imaging geometry to obtain best depth perception with minimal eyestrain. In general, a larger stereoscopic shift produces improved depth perception; however, as the shift increases, it becomes more difficult for the observer to fuse the images for the stereoscopic effect, and eye fatigue increases. According to Christensen's *Physics of Diagnostic Radiology* (Curry *et al*, 1992), early radiologists determined empirically that a tube shift of 10% of the source-to-film distance worked well. This translates to a stereo shift angle of about $\pm 3^{\circ}$ ($\tan^{-1}(0.05) \cong 3^{\circ}$) relative to a normal to the detector.

Stereoscopic imaging has not achieved widespread acceptance in clinical practice, mainly because of the doubled film cost and increased patient exposure (Curry *et al*, 1992). A secondary problem is the need to train the eyes to perceive the stereoscopic effect without aid, or to use a special stereoscope, with careful arrangement of the films. Digital imaging may make the stereoscopic technique a viable approach because no additional film cost will be required. Furthermore, a digital detector has a wider linear-response range and a higher contrast sensitivity than a screen-film system so that good-quality images may be acquired at a reduced radiation dose. Images in digital form can be subjected to image processing, further enhancing the visibility of the image details. Digital stereoscopic images can be viewed on a single electronic display device that displays the left-eye and right-eye images alternately at a high refresh rate. The observer views the displayed images through a stereo goggle such as a pair of liquid crystal display (LCD) glasses. The LCD panels act as electronic shutters, blocking the light to the left eye and the right eye alternately. When the goggle is synchronized with the display so that only the left eye can see the left-eye image and only the right eye can see the right-eye image in rapid succession, the parallax between the two images will create a stereo effect. The stereoscopic images can be viewed singly in the conventional manner or stereoscopically on the same viewing station to provide complementary diagnostic information.

An additional advantage of stereoscopic imaging is the 3-dimensional (3D) information it provides on the lesions of interest. It has been reported that the 3D distribution of microcalcifications may be correlated with the malignant or benign nature of the cluster (Conant *et al*, 1996; Maidment *et al*, 1996). Spiculations from a mass may be more readily distinguished from overlapping tissues under stereoscopic viewing conditions. This supplementary diagnostic information may improve the classification of malignant and benign lesions, thereby reducing unnecessary biopsies and increasing the positive predictive value of mammography.

We are evaluating the application of stereoscopic techniques to digital mammography. Previously we studied the effects of stereo shift and imaging conditions on the depth perception of fibrils in stereo phantom images (Chan *et al*, 2001). We also demonstrated that a virtual cursor could provide accurate depth measurements in stereo phantom images acquired under mammographic conditions (Goodsitt *et al*, 2000; Goodsitt *et al*, 2002). In the present study, we further evaluated the effects of geometric magnification, display zooming, and x-ray exposure on the visual depth discrimination of fibril-like objects in stereo phantom mammograms.

2. MATERIALS AND METHODS

2.1 Modular Stereo Phantom

We have designed a modular stereo phantom for evaluation of depth perception in stereomammography. A schematic of the phantom is shown in Fig. 2. The phantom consists of six 1-mm-thick Lexan sheets, each separated by 1-mm-thick spacers. Each Lexan plate contains a 5 X 5 array of object areas. Fifty nylon fibrils, each about 8-mm in length and 0.53 mm in diameter, are arranged in these object areas. Twenty-five fibrils are oriented perpendicular and another 25 are oriented parallel to the stereo shift direction. Henceforth, we will refer to the fibrils oriented in the perpendicular direction as "vertical" and the fibrils oriented in the parallel direction as "horizontal." On average, eight to nine fibrils are placed in the object areas on each Lexan plate. The location and orientation of a fibril on a Lexan plate are randomly chosen with the constraint that, in the projection image, each object area contains the projection of one vertical and one horizontal fibril that cross each other. These plates can be arranged in different orders to produce many independent object configurations, i.e., the depth separation and whether the vertical fibril is in the front of or behind the horizontal fibril in a given pair change when the order of the plates changes. Different types of test objects such as microcalcifications may be used in place of the fibrils to generate a different phantom although only fibrils were used in the present study. An additional 1-mm-thick Lexan plate without objects is placed on top of the phantom to protect the test objects on the top layer. The total thickness of Lexan in the phantom is therefore 7 mm.

2.2 Image Acquisition and Display

Digital stereoscopic image pairs were acquired with a GE Senographe 2000D digital mammography system. The system employs a digital detector consisting of a CsI:Tl scintillator and an amorphous-Si active matrix flat panel. The detector measures 23 cm x 18 cm, with a pixel size of 100 μm x 100 μm. We acquired stereoscopic pairs of images using x-ray techniques of 30 kVp, Rh target/Rh filter, a ±3° stereo-angle, contact (reciprocating grid, 0.3 mm focal spot) and 1.8X magnification (no grid, 0.15 mm focal spot) geometries, and exposures of 4, 8, 32, and 63 mAs per image. A relatively hard x-ray beam was used to produce lower contrast images, thus making the perception task more challenging.

Since the digital mammography system was not designed for stereo imaging, it is not easy to move the x-ray focal spot to the angulated positions at ±3° from the central ray for imaging the stereo pair. We used an equivalent imaging geometry (Fig. 1) in which the phantom was shifted instead of the x-ray source. Comparing the two geometries in Fig. 1, it can be seen that the position of the x-ray source relative to the phantom is the same except that the focal-spot-to-detector distance is slightly shorter in the phantom-shift geometry because the x-ray source moves along an arc. However, with the 3° shift about a fulcrum of rotation at a distance of 46 cm from the x-ray focal spot, this error is less than 0.1%. Using the geometry of the x-ray system, we calculated that a $\pm 3^{\circ}$ stereo shift of the x-ray focal spot is equivalent to a phantom shift distance of ± 2.4 cm from its central position. The shift distance is the same for either the contact geometry or the magnification geometry.

We built a phantom platform with Lexan (Fig. 3) to move the phantom from one position to the other in a direction parallel to the chest wall for acquisition of the stereo pair. The platform has a stationary base that is fitted on the Bucky holder for contact geometry or on the magnification stand for magnification geometry. A sliding plate on top of the base is used to support and move the phantom parallel to the chest wall direction of the mammography system. The sliding plate is guided by two guardrails parallel to the chest wall to ensure a precise and reproducible movement. The total thickness of the Lexan platform is 1.7 cm. During image acquisition, care was taken such that the phantom remained stationary on the sliding plate while the plate was moved between the two shifted positions. Pictures of the phantom platform at the left and right shifted positions in the contact geometry are shown in Fig. 3.

Three different configurations of the fibril phantoms were imaged under each exposure condition. Twenty-four (= 3 phantoms X 4 exposures X 2 geometries) stereo image pairs were thus produced. For each exposure and geometry condition, there were a total of 75 pairs of fibril images (25 fibril pairs in each phantom configuration x 3 configurations) at 5 different depth separations (2, 4, 6, 8, 10 mm) to be evaluated. An example of a stereo image pair acquired with contact geometry is shown in Fig. 4.

The images were displayed on a 21" Barco-Metheus (Beaverton, OR) model 521 display monitor driven by a Barco-Metheus model 1760S stereoscopic board and a SUN

Microsystems (Palo Alto, CA) Ultra 10 computer using in-house developed software. The Metheus board displays 1408 x 1408 x 8 bit images at a refresh rate of 114 Hz. It operates in a page flipping stereoscopic mode with the left- and right-eye images displayed alternately. NuVision (Beaverton, OR) LCD stereoscopic glasses were used for viewing the stereoscopic images. The stereo workstation is shown in Fig. 5.

2.3 Observer Experiment

Five observers including two experienced mammographic radiologists participated in the experiment. All observers took a standard Randot Circles Stereo test (Stereo Optical Co., Inc., Chicago, IL) to evaluate their stereo acuity. In this test, the observers viewed ten rows of test objects through polarized glasses. Each row contains 3 objects, one of which is the object that exhibits the stereo effect and appears to be on a plane different from the other two objects. The difference progressively decreases due to decreasing stereo shift, and thus increasing the degree of difficulty. The observers had to determine which one was the stereo object in each row. All of our observers could correctly identify all the objects in the test, indicating that their stereo acuity was at least 20 sec of arc at a viewing distance of 16". Their performance is comparable to the average performance (21.3 sec of arc) for adults with excellent, balanced monocular visual acuity measured with this test pattern (Simons, 1981).

For our experiment, the task for the observers was to visually judge whether the vertical fibril in each pair of overlapping fibrils was in front of (closer to the observer) or behind the horizontal fibril. The observer was not informed of the truth after reading each image. Each observer read the images sequentially in a different randomized order. The reading order of the fibril pairs in the 5 X 5 matrix in a given image was changed randomly by changing the starting location and the reading direction, e.g., from the upper left corner and by row, from the upper left corner and by column, from the lower right corner and by row, etc., in an effort to further reduce any potential effects of memorization. The contact images were read in two modes – in a regular and in a 2X-zoom mode, referred to as the contact and contact-zoom mode, respectively. The 1.8X geometric magnification images were read only in the regular mode, referred to as the magnification mode. The contact and the contact-zoom modes of the same image were not read consecutively so that it was unlikely that the observer would remember the results of the other mode. The observers were not informed of the conditions under which the image being viewed was acquired, although the difference in image sizes between the contact and the magnification or contact-zoom images were apparent. Prior to reading the test cases, the observers participated in training sessions to become familiar with the reading task.

3. RESULTS

In this study, we quantified the accuracy of depth perception in stereo images by an observer as the percentage of correct decisions to differentiate the relative depths of the fibrils. The results were averaged over the 5 observers. The dependences of the average percentage of correct decisions on the depth separation of the crossing fibrils and the exposure levels for the contact, contact-zoom, and magnification modes are shown in Fig. 6(a) to Fig. 6(c), respectively. Generally, the percentage of correct decisions increases as the exposure increases and as the depth separation between the two fibrils increases. The dependence on the depth separation diminishes as the exposure increases. At small depth separations, the noise in the images has a much stronger influence on the depth perception. The percentage of correct decisions increases rapidly as the exposure increases. At a depth separation of 10 mm, the percentage of correct decisions was 100% for all observers in all three modes, regardless of exposure levels. The curves for contact mode are very similar to those for the contact-zoom mode. On the other hand, the curves for the magnification mode are much higher than those of the contact or contact-zoom mode. The standard deviation of the percentage of correct decisions varied from 0 to about 13% for the contact mode and the contact-zoom mode, and varied from 0 to 6.7% for the magnification mode. The standard deviation generally increased as the percentage of correct decisions decreased. The standard deviation was zero for the conditions in which the average percentage of correct decisions was 100% because all observers were 100% correct in their decisions.

The statistical significance of the differences between every two modes, contact vs contact-zoom, contact vs magnification, and contact-zoom vs magnification, was estimated by a two-tailed paired-t test. The paired t-test was performed for each depth separation and exposure level over the 5 observers. The p-values for the contact-vs-magnification and contact-zoom-vs-magnification for the various exposure and depth separation conditions are shown in Table 1 and Table 2, respectively. The differences between the contact and the magnification modes are statistically significant (p value<0.05) for depth separations of 2 mm to 6 mm at 4 mAs, and for a 2-mm separation at 8 mAs. The differences between the contact-zoom and the magnification modes are statistically significant for depth separations of 2 mm to 6 mm at 4 mAs, for 2-mm to 4-mm separations at 8 mAs, and for a 2-mm separation at 32 mAs. The differences between the contact and contact-zoom modes are not statistically significant.

We further analyzed separately the reading results for two subgroups of crossing fibrils, one subgroup with the vertical fibril in front of (referred to as the "front group") and the other behind (referred to as the "back group") the horizontal fibril. The average percentage of correct decisions as a function of depth separation was obtained for each exposure level, similar to the analysis for the entire group described above. We observed that the average percentage of correct decisions for the front group was often greater than that for the back group for a given exposure and a given depth separation. A histogram of the differences between the average percentage of correct decisions for the front group and that for the back group under the corresponding conditions is plotted in Fig. 7 for the 60 conditions studied (4 exposure levels X 5 depth separations X 3 modes). Of the 60 differences, only three were negative, i.e., the average percentage of correct decisions for the front group was smaller than that for the back group. All 28 zeroes (no difference) happened when both the front group and the back group were 100% correct. These occurred when the depth separations were large and the exposures were high. The other 29 differences were positive, i.e., the percentage of correct decisions for the front group was larger than that for the back group. However, paired t-tests of the differences between the front and the back group under each condition did not reach statistical significance, probably due to the smaller numbers of samples when they were separated into subgroups.

4. DISCUSSION

Depth perception in stereomammography depends on a number of factors including the x-ray exposure, depth separation, and imaging geometry. In this study, we investigated the dependence of the percentage of correct decisions in differentiating the relative depths of two crossing fibrils on these factors using images acquired with ±3° stereo angle. We found that a 2-mm depth resolution could be achieved with over 60% accuracy for all imaging conditions studied. For contact geometry, the accuracy improved to greater than 90% at higher exposures. Magnification stereomammography provided over 90% accuracy at a 2-mm depth resolution for all exposure levels studied. An interesting finding was that displaying the stereo images acquired with contact geometry in 2X zoom mode did not improve the depth discrimination accuracy. In contrast, geometric magnification with about the same factor (1.8X) of enlargement significantly improved depth perception. This result indicated that the signal-to-noise ratio (SNR) might be a more important factor affecting depth perception than the perceived object size. When the images are acquired with geometric magnification, both the spatial resolution of the detector relative to the object and the x-ray quanta per unit object area increase (Doi and Rossmann, 1974; Doi and Imhof, 1977), although geometric unsharpness may somewhat reduce the gain in resolution. The improved detector resolution and reduced quantum mottle contributed to an increase in the SNR of the image. On the other hand, if the images were acquired in contact geometry and the object size was enlarged electronically by zooming during display, the inherent SNR of the object in the images remained fixed. The differences in the perceived SNRs (Loo *et al*, 1985; Aufrichtig, 1999) between the contact mode and the contact-zoom mode would be mainly caused by the change in the perceived noise of the display monitor relative to the object size as well as the change in the perceived signal and image noise spectra due to zooming relative to the frequency response of the observer's visual system. Display zooming may have a strong influence if the perception is limited by the resolution of the human visual system. In our case, the objects were relatively large and it was unlikely that they were near the resolution limit of the observers' visual system. The improved SNR inherent in the geometrically magnified images may therefore have a dominant effect on depth discrimination compared with that of increased displayed object size. This may be the reason that display zoom did not have a strong impact on the accuracy of depth perception in this study.

We plotted the average percentage of correct decisions as a function of log exposure (mAs) for each depth separation between the two crossing fibrils in the pair as shown in Fig. 8(a) and 8(b), respectively, for the contact and contact-zoom modes. The average percentages of correct decisions for the magnification mode under all conditions were greater than 90% and were not plotted. Three of the data points at a 8-mm depth separation appear to be lower than those at a 6-mm depth separation for a given exposure. Since the standard deviation at each of these data points is about twice as large as the difference between the percentage of correct decisions at 6-mm and 8-mm separations, the apparent local reverse of the trend can likely be attributed to experimental uncertainties. From the curves of the contact and contact-zoom modes, it appears that there is no simple relationship between the percentage of correct decisions and log exposure. The curve shape varied among the different depth separations and they were not linear. The percentage of correct decisions increased with exposure more rapidly at low dose levels and leveled off at high doses. Depth discrimination is different from a single-object detection task. The relationships among the perceived depth separation, the SNR's of the individual objects, and the percentage of correct decisions are still unknown. Further studies are needed to explore how depth discrimination is related to the SNR of the individual objects and if the depth discrimination task can be predicted by SNR models.

The intraobserver variability was estimated from two repeated readings of the set of test images by one observer. The difference between the two readings for each exposure level and depth separation was calculated. The difference in the percentage of correct decisions between the two readings varied from 0 to 20%, from 0 to 8%, and from 0 to 8%, respectively, for the contact, contact-zoom, and magnification modes. The variability generally increased with decreasing depth separation and decreasing exposure. There were no differences between the two readings at depth separations of 8 mm and 10 mm for all exposure levels and all image modes. For the magnification mode, the two repeated readings were identical for 18 of the 20 conditions (5 depth separations and 4 exposure levels). A difference was observed only at a 2-mm separation with the two lower exposure levels, 4 mAs and 8 mAs. For both the contact and contact-zoom modes, 14 of the 20 conditions were identical. Four of the 6 differences occurred at a 2-mm separation with the four exposure levels (4, 8, 32, 63 mAs).

In a previous study, we designed a virtual cursor to measure the absolute depths of the fibrils in stereo phantom images similar to those used in this study. We found that the accuracy of the absolute depth measurement also depended on the image modes. The accuracy of the measurements in contact-zoom mode was similar to those in contact mode, whereas the accuracy was higher when measured in the images acquired with geometric magnification (Goodsitt *et al*, 2002). These results are consistent with the observation in the current depth perception experiments.

5. CONCLUSIONS

The accuracy of depth discrimination of fibrils in stereomammography increases with x-ray exposure and depth separation and depends on imaging geometry. At a stereo angle of ±3°, a 2-mm depth resolution was achieved with over 60% accuracy for all imaging conditions studied. It improved to greater than 90% accuracy at higher doses in contact geometry. With magnification stereomammography, a 2-mm depth resolution was achieved with greater than 90% accuracy for all exposure levels studied. It was found that zooming the contact stereo images by 2X did not improve the accuracy under our experimental conditions. When the images were noisy and the depth separation between the fibrils was small, depth discrimination was significantly better in stereo images acquired with geometric magnification than in images acquired with a contact technique and displayed with or without zooming. These results indicate that stereoscopic imaging, and in particular, magnification stereomammography, may be useful for visualizing the spatial distribution of microcalcifications in a cluster and differentiating overlapping tissues from masses on mammograms. Further studies are underway to investigate the dependence of depth perception on the shape and size of the objects and to evaluate if specially designed cursors can assist in depth discrimination of target objects in stereoscopic images. An observer experiment is being conducted to evaluate the characterization of mammographic lesions in stereo images of biopsy tissue specimens.

ACKNOWLEDGMENTS

This work is supported by U. S. Army Medical Research and Materiel Command Grants DAMD 17-98-1-8210 and DAMD17-99-1-9294. The content of this publication does not necessarily reflect the position of the funding agency, and no official endorsement of any equipment and product of any companies mentioned in this publication should be inferred.

REFERENCES

Aufrichtig R 1999 Comparison of low contrast detectability between a digital amorphous silicon and a screen-film based imaging system for thoracic radiography. Medical Physics **26** 1349-1358.

Beam C A, Layde P M and Sullivan D C 1996 Variability in the interpretation of screening mammograms by US radiologists - Findings from a national sample. Archives Internal Medicine **156** 209-213.

Bird R E, Wallace T W and Yankaskas B C 1992 Analysis of cancers missed at screening mammography. Radiology **184** 613-617.

Boone J M, Nelson T R, Lindfors K K and Seibert J A 2001 Dedicated breast CT: Radiation dose and image quality evaluation. Radiology **221** 657-667.

Chan H P, Goodsitt M M, Darner K L, Sullivan J M, Hadjiiski L M, Petrick N and Sahiner B 2001 Effects of stereoscopic imaging technique on depth discrimination. In: M. J. Yaffe (Ed.) Proc. IWDM 2000- 5th International Workshop on Digital Mammography, Digital Mammography 13-18. Toronto, Canada: (City: Medical Physics Publishing, Madison, WI).

Conant E F, Maidment A D, Albert M, Piccoli C W, Nussbaum S A and McCue P A 1996 Small field-of-view digital imaging of breast calcifications: method to improve diagnostic specificity. Radiology **201(P)** 369.

Curry T S, Dowdey J E and Murry R C 1992*Christensen's Physics of Diagnostic Radiology.* (Fourth ed.) (Philadelphia, PA: Lea & Febiger).

Doi K and Duda E E 1983 Detectability of depth information by use of magnification stereoscopic technique in cerebral angiography. Radiology **146** 91-95.

Doi K and Imhof H 1977 Noise reduction by radiographic magnification. Radiology **122** 479-487.

Doi K, Patronas N J, Duda E E, Geldner E and Dietz K 1981 X-ray imaging of blood vessels to the brain by use of magnification stereoscopic technique. Advance in Neurology **30** 175-189.

Doi K and Rossmann K 1974 The effect of radiographic magnification on blood vessel imaging with various screen-film systems. Medical Physics **1** 257-261.

Getty D J, Pickett R M and D'Orsi C J 2001 Stereoscopic digital mammography: improving detection and diagnosis of breast cancer. In: H. U. Lemke, M. W. Vannier, K. Inamura, A. G. Farman, & K. Doi (Eds.) Computer Assisted Radiology and Surgery 2001, Proc. 15th International Congress and Exhibition, International Congress Series 1230 506-511. Berlin: (City: Elsevier, Amsterdam).

Goodsitt M M, Chan H P, Darner K L and Hadjiiski L M 2002 The effects of stereo shift angle, geometric magnification and display zoom on depth measurements in digital stereomammography. Medical Physics **29** 2725-2734.

Goodsitt M M, Chan H P and Hadjiiski L M 2000 Stereomammography: Evaluation of depth perception using a virtual 3D cursor. Medical Physics **27** 1305-1310.

Harvey J A, Fajardo L L and Innis C A 1993 Previous mammograms in patients with impalpable breast carcinomas: Retrospective vs blinded interpretation. American Journal of Roentgenology **161** 1167-1172.

Higashida Y, Hirata Y, Saito R, Doudanuki S, Bussaka H and Takahashi M 1988 Depth determination on stereoscopic digital subtraction angiograms. Radiology **168** 560-562.

Jackson V P, Hendrick R E, Feig S A and Kopans D B 1993 Imaging of the radiographically dense breast. Radiology **188** 297-301.

Kelsey C A, Moseley R D, Mettler S A and Briscoe D E 1982 Cost-effectiveness of stereoscopic radiographs in detection of lung nodules. Radiology **142** 611-613.

Loo L N, Doi K and Metz C E 1985 Investigation of basic imaging properties in digital radiography. 4. Effect of unsharp masking on the detectability of simple patterns. Medical Physics **12** 209-214.

Maidment A D A, Albert M, Conant E F, Piccoli C W and McCue P A 1996 Prototype workstation for 3-D diagnosis of breast calcifications. Radiology **201(P)** 556.

Maidment A D A, Bakic P and Alberg M 2003 Is stereomammography possible without increasing dose? In: H. Petitgen (Ed.) Proc. IWDM 2002- 6th International Workshop on Digital Mammography, Digital Mammography 510-515. Bremen, Germany: (City: Springer-Verlag, Berlin, New York).

Niklason L T, Christian B T, Niklason L E, Kopans D B, Castleberry D E, Opsahl-Ong B H, Landberg C E, Slanetz P J and al. e 1997 Digital tomosynthesis in breast imaging. Radiology **205** 399-406.

Ragnarsson J I and Karrholm J 1992 Factors influencing postoperative movement in displaced femoral neck fractures: evaluation by conventional radiography and stereoradiography. J. Orthop Trauma **6** 152-158.

Raptopoulos V, Baum J K, Hochman M, Karellas A, Houlihan M J and D'Orsi C J 1996 High resolution CT mammography of surgical biopsy specimens. J. Computer Assisted Tomography **20** 179-184.

Seidman H, Gelb S K, Silverberg E, LaVerda N and Lubera J A 1987 Survival experience in the Breast Cancer Detection Demonstration Project. CA Cancer J Clin. **37** 258-290.

Simons K 1981 Stereoacuity norms in young children. Arch. Opthalmol. **99** 435-445.

Suryanarayanan S, Karellas A, Vedantham S, Glick S J, D'Orsi C J, Baker S P and Webber R L 2000 Comparison of tomosynthesis methods used with digital mammography. Academic Radiology **7** 1085-1097.

Trocme M C, Sather A H and An K N 1990 A biplanar cephalometric stereoradiography technique. Am. J. Orthodontics and Dentofacial Orthopedics **98** 168-175.

Wallis M G, Walsh M T and Lee J R 1991 A review of false negative mammography in a symptomatic population. Clinical Radiology **44** 13-15.

Table 1. The p-values from the two-tailed paired t-test of the differences in the percentage of correct decisions in differentiating the depths of two crossing fibrils between the contact and the magnification mode. The entries indicated by "—" have p-values > 0.05 so that the differences are not statistically significant. The two entries indicated by —* have p-values of 0.089 and 0.065, close to being significant.

Depth Separation	Exposure			
(mm)	4 mAs	8 mAs	32 mAs	63 mAs
2	0.007	0.000	—*	—
4	0.009	—*	—	—
6	0.034	—	—	—
8	—	—	—	—
10	—	—	—	—

Table 2. The p-values from the two-tailed paired t-test of the differences in the percentage of correct decisions in differentiating the depths of two crossing fibrils between the contact-zoom and the magnification mode. The entries indicated by "—" have p-values > 0.05 so that the differences are not statistically significant.

Depth Separation	Exposure			
(mm)	4 mAs	8 mAs	32 mAs	63 mAs
2	0.014	0.003	0.011	—
4	0.016	0.003	—	—
6	0.021	—	—	—
8	—	—	—	—
10	—	—	—	—

FIGURE CAPTIONS

Fig. 1. Imaging geometry for acquisition of stereoscopic image pairs. On the left is a conventional "focal-spot-shift" method in which the focal spot is shifted to the left and to the right by a distance of w to expose the left-eye and right-eye images. On the right is an equivalent "phantom-shift" method in which the phantom is shifted to the left and the right of the central ray by a distance of w. The "phantom (R)" geometry corresponds to the "f.s. (R)" geometry, and the "phantom (L)" geometry corresponds to the "f.s. (L)" geometry.

Fig. 2. A modular stereo phantom consists of six layers of Lexan plates on which nylon fibrils were pasted either in the horizontal or the vertical direction in one of the 5X5 matrix locations on one of the plates. By properly arranging 50 fibrils on the six plates, the projected image will contain 25 pairs of crossing fibrils with different depth separations between the two fibrils.

Fig. 3. The phantom platform placed on top of the detector of the digital mammography system in the setup for contact imaging. The sliding plate with the stereo phantom was shifted to the left in (a) and to the right in (b) at a distance equivalent to a $\pm 3^{\circ}$ stereo angle.

Fig. 4. A stereo image pair acquired in contact geometry: (a) left-eye image, (b) right-eye image, (c) displayed stereo image - the 25 pairs of crossing fibrils showed different degrees of stereo shift due to the different depth separations between the two fibrils.

Fig. 5. The SUN-based Barco-Metheus stereo display workstation used in the observer study.

Fig. 6. Percentage of correct decisions in differentiating the relative depths of two crossing fibrils, averaged over 5 observers. (a) Stereo images acquired with contact geometry, (b) Stereo images acquired with contact geometry, displayed

with 2X zoom, and (c) Stereo images acquired with 1.8X geometric magnification.

Fig. 7. Histogram of the difference in the percentage of correct decisions between the front group (vertical fibril in front of horizontal fibril) and the back group (vertical fibril behind horizontal fibril).

Fig. 8. Dependence of the percentage of correction decisions on the logarithm of exposure. (a) Contact mode. (b) Contact-zoom mode.

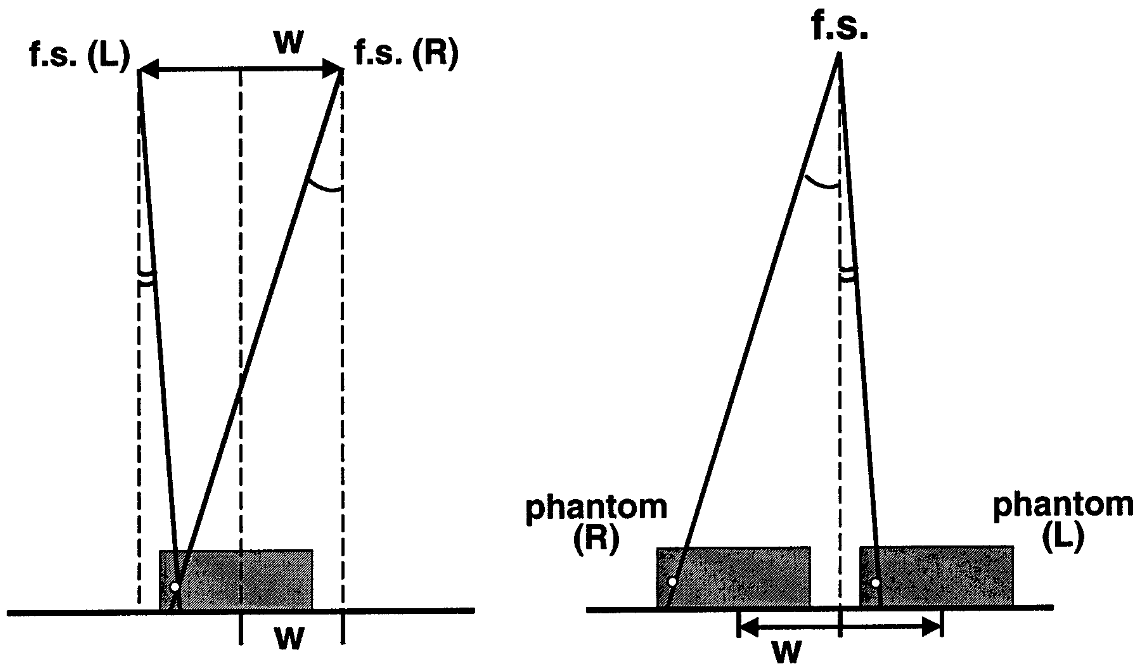

Fig. 1. Imaging geometry for acquisition of stereoscopic image pairs. On the left is a conventional "focal-spot-shift" method in which the focal spot is shifted to the left and to the right by a distance of w to expose the left-eye and right-eye images. On the right is an equivalent "phantom-shift" method in which the phantom is shifted to the left and the right of the central ray by a distance of w. The "phantom (R)" geometry corresponds to the "f.s. (R)" geometry, and the "phantom (L)" geometry corresponds to the "f.s. (L)" geometry.

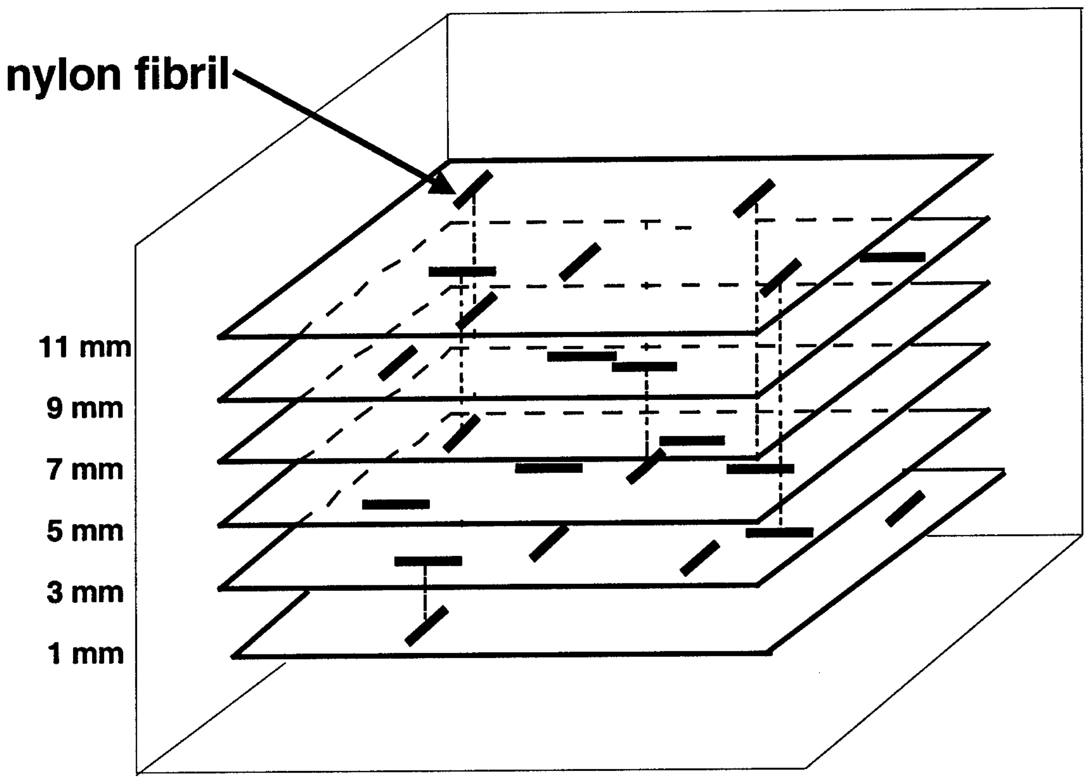

Fig. 2. A modular stereo phantom consists of six layers of Lexan plates on which nylon fibrils were pasted either in the horizontal or the vertical direction in one of the 5X5 matrix locations on one of the plates. By properly arranging 50 fibrils on the six plates, the projected image will contain 25 pairs of crossing fibrils with different depth separations between the two fibrils.

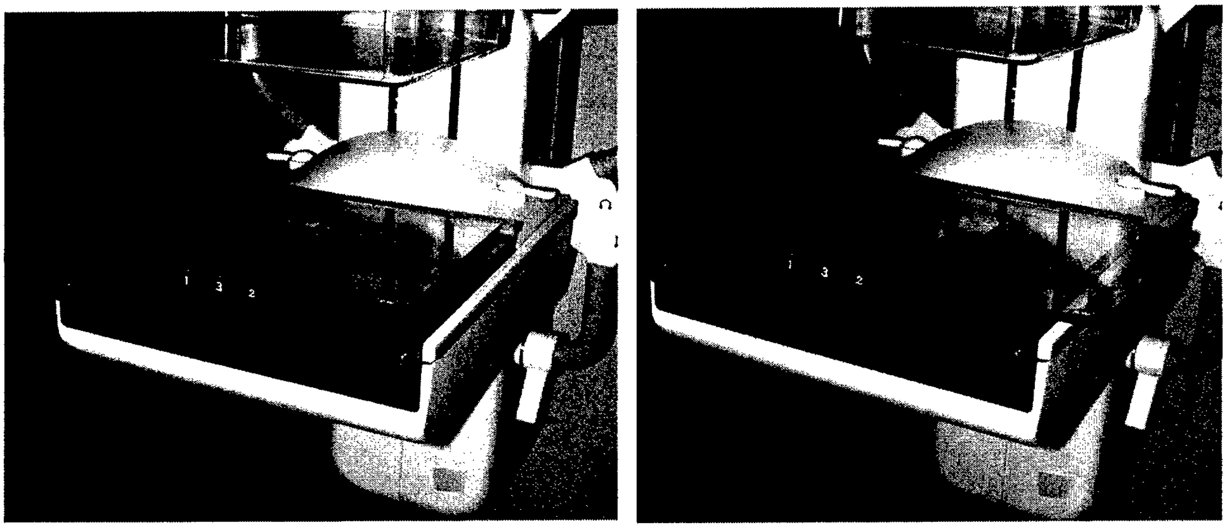

(a) (b)

Fig. 3. The phantom platform placed on top of the detector of the digital mammography system in the setup for contact imaging. The sliding plate with the stereo phantom was shifted to the left in (a) and to the right in (b) at a distance equivalent to a ±3° stereo angle.

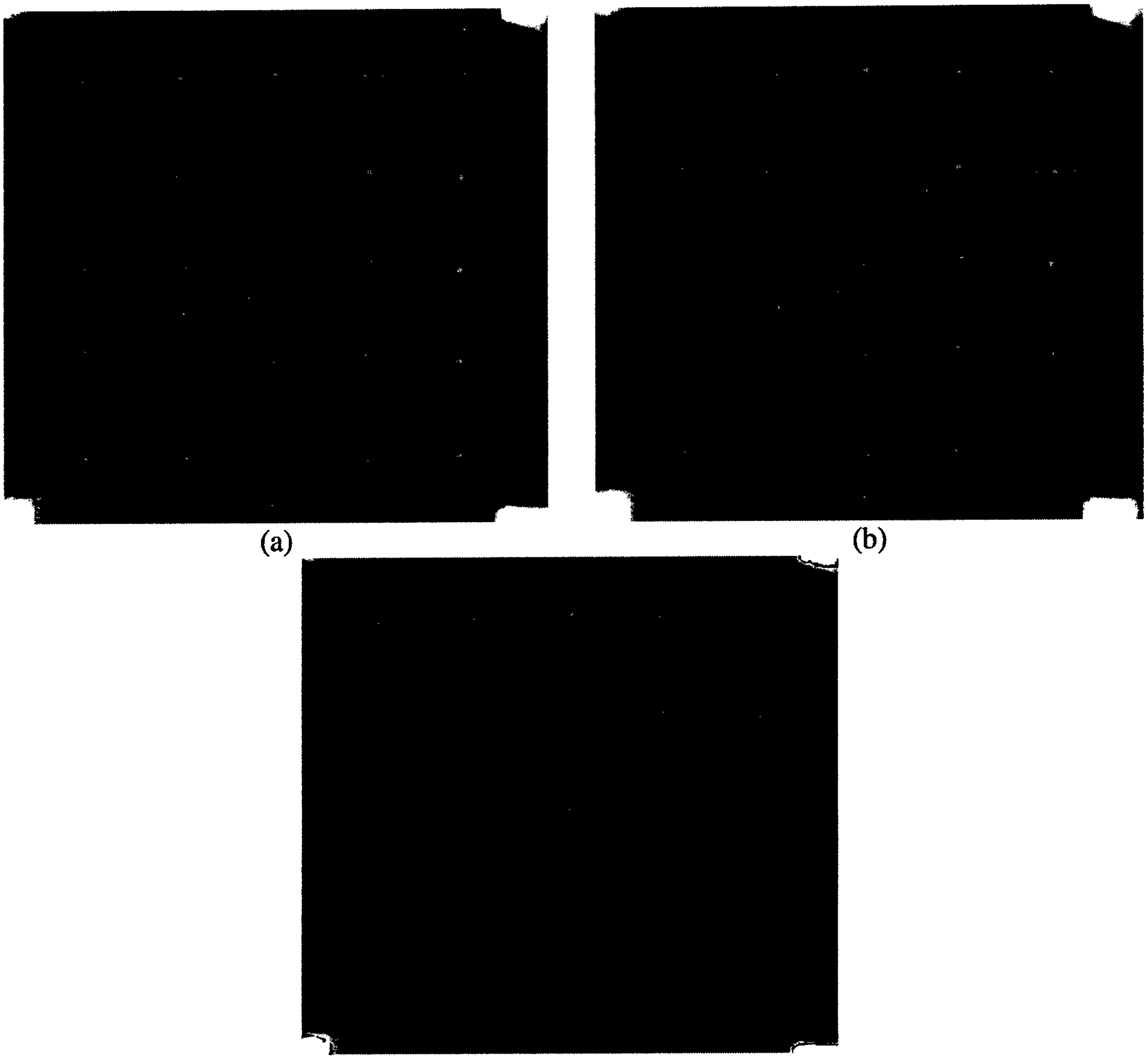

(a) (b) (c)

Fig. 4. A stereo image pair acquired in contact geometry: (a) left-eye image, (b) right-eye image, (c) displayed stereo image - the 25 pairs of crossing fibrils showed different degrees of stereo shift due to the different depth separations between the two fibrils.

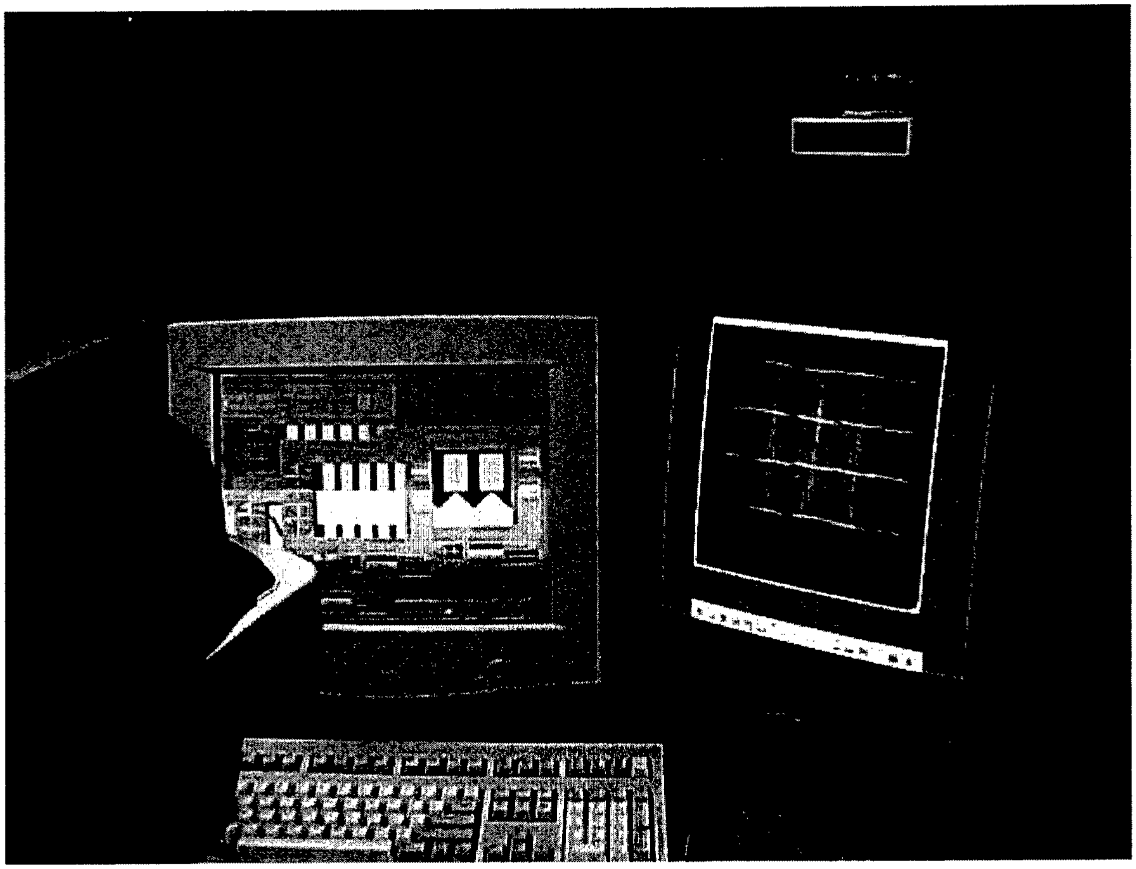

Fig. 5. The SUN-based Barco-Metheus stereo display workstation used in the observer study.

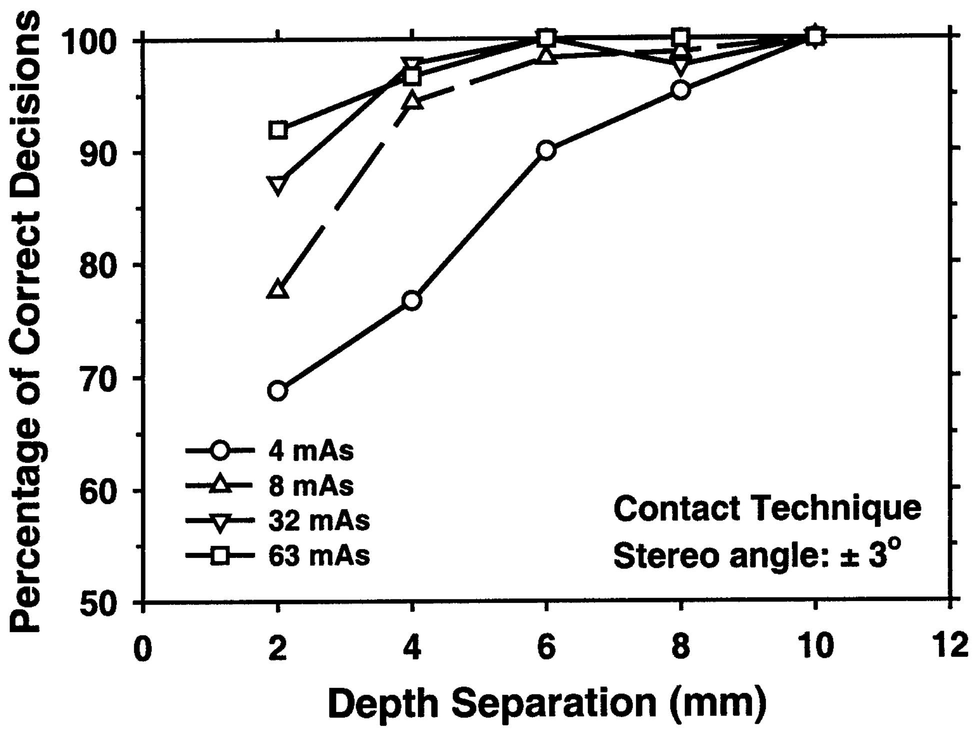
Percentage of Correct Decisions
100
90
80
70
60
50
0
2
4
6
8
10
12
Depth Separation (mm)
4 mAs
8 mAs
32 mAs
63 mAs
Contact Technique
Stereo angle: ± 3°

(a)

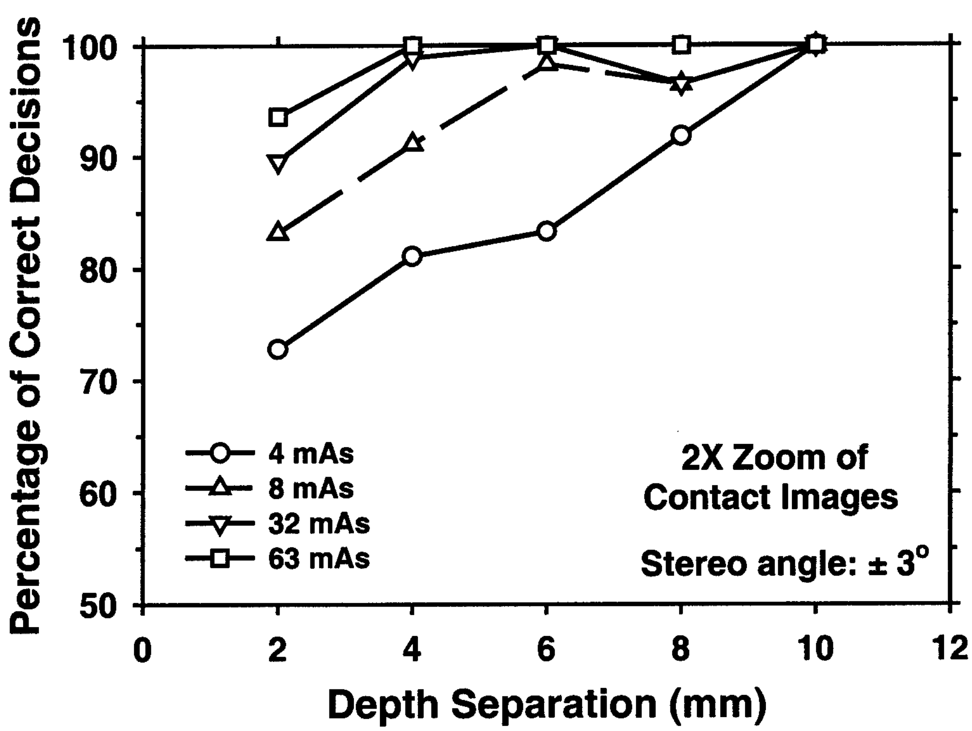
Percentage of Correct Decisions
100
90
80
70
60
50
0
2
4
6
8
10
12
Depth Separation (mm)
4 mAs
8 mAs
32 mAs
63 mAs
2X Zoom of
Contact Images
Stereo angle: ± 3°

(b)

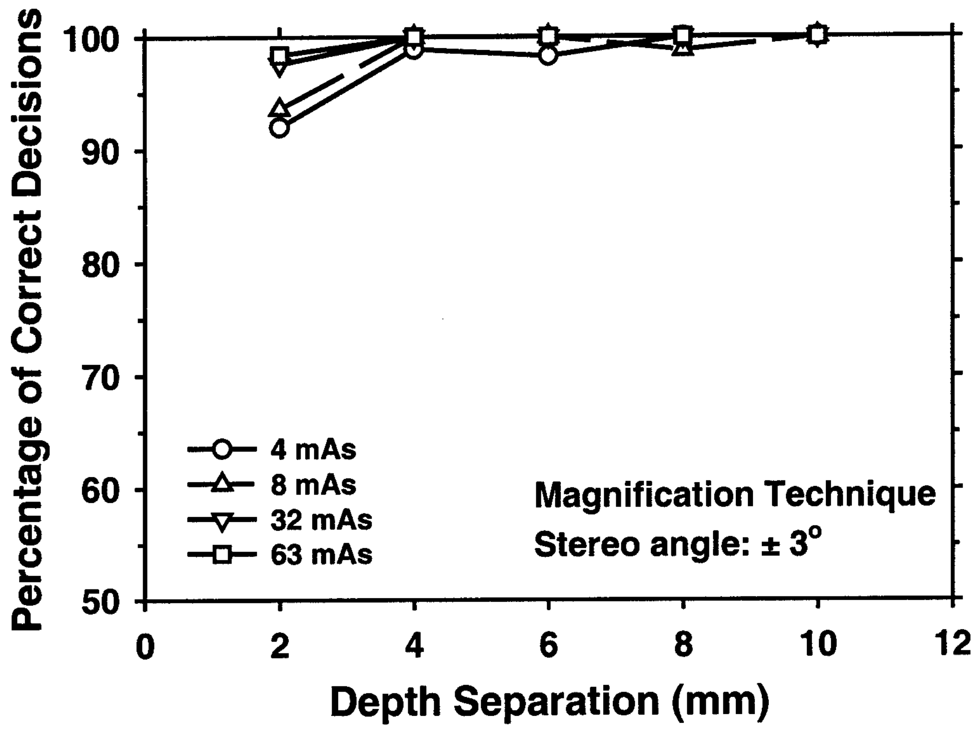

(c)

Fig. 6. Percentage of correct decisions in differentiating the relative depths of two crossing fibrils, averaged over 5 observers. (a) Stereo images acquired with contact geometry, (b) Stereo images acquired with contact geometry, displayed with 2X zoom, and (c) Stereo images acquired with 1.8X geometric magnification.

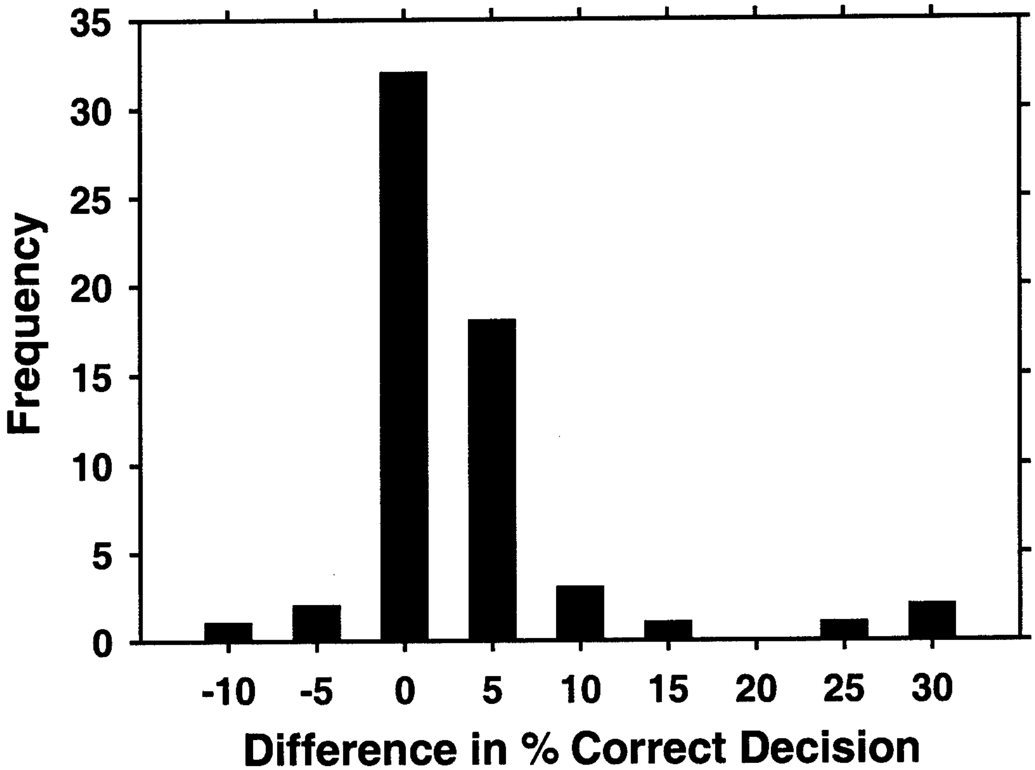

Fig. 7. Histogram of the difference in the percentage of correct decisions between the front group (vertical fibril in front of horizontal fibril) and the back group (vertical fibril behind horizontal fibril).

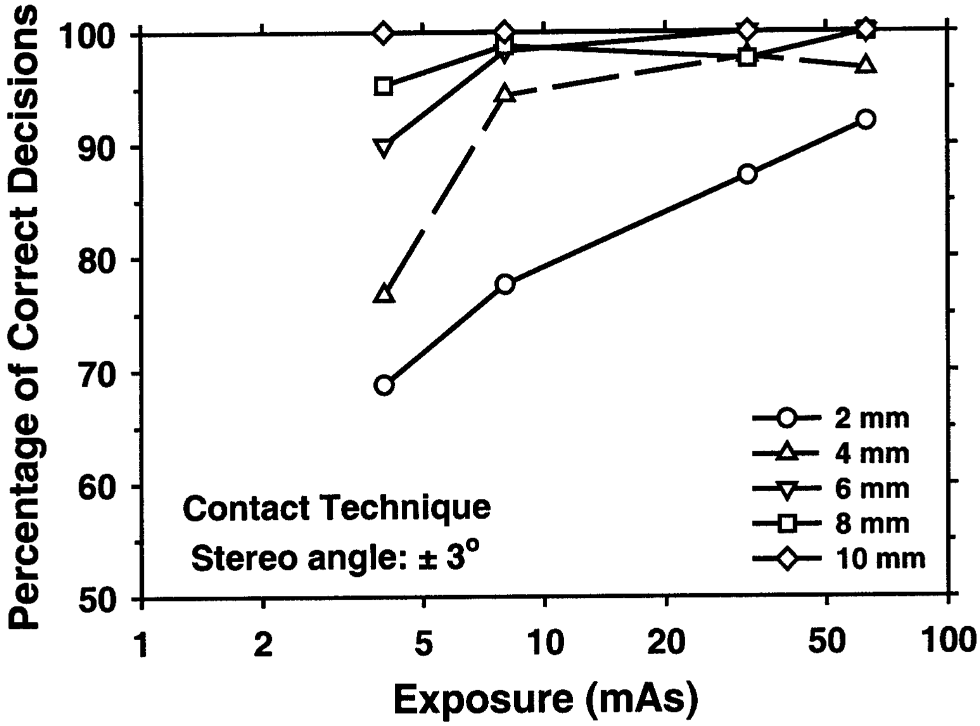

(a)

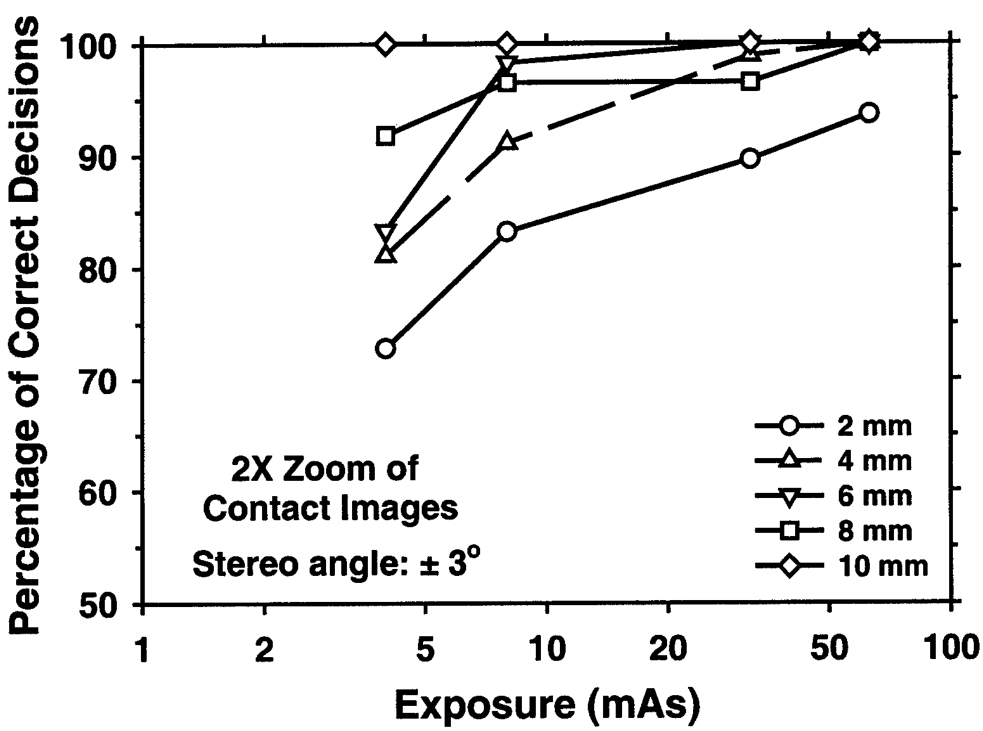

(b)

Fig. 8. Dependence of the percentage of correction decisions on the logarithm of exposure. (a) Contact mode. (b) Contact-zoom mode.

the classification of the microcalcification. The two observers with 3 and 12 years in a specialized department with at least 12,000 mammograms per year have almost the same accuracy in the discrimination of malignant or benign calcifications, and the intraobserver-variability shows no difference between FFS and SP1. Contour enhancement showed no advantage, either in the size of the cluster or in the accuracy. The accuracy was worse in the images after postprocessing. This can be explained by the fact that every postprocessing procedure makes the MTF of the system worse. The form of the microcalcification gets lost by edge enhancing and so the diagnosis is much more difficult.

In summary we can say that digital luminescence mammography is equal to film-screen systems not only in phantom studies (Fiedler et al. 1999, Cowen et al. 1997) but in analysis of microcalcifications too. The advantages of digital techniques like archiving, teleradiology, and probably lower dose will be available in the future in high quality mammography.

REFERENCES

Cowen, A. R., J. H. Launders, M. Jadav, and D. S. Brettler (1997). "Visibility of microcalcifications in computed and screen-film mammography." *Phys. Med. Biol.* 42: 1533–1548.

Fiedler, E., U. Aichinger, C. Böhner, M. Säbel, R. Schulz-Wendtland, and W. Bautz (1999). "Bildgüte und Strahlenexposition bei der Digitalen Mammographie mit Speicherfolien in Vergrößerungstechnik." *RöFo* 171: 60–64.

Karssemeijer, N., J. T. M. Frieing, and H. C. L. Hendriks (1993). "Spatial resolution in digital mammography." *Invest. Radiol.* 28: 413–419.

Effects of Stereoscopic Imaging Technique on Depth Discrimination

HEANG-PING CHAN
MITCHELL M. GOODSITT
KATIE L. DARNER
JEFFREY M. SULLIVAN
LUDOMIR M. HADJIISKI
NICHOLAS PETRICK
BERKMAN SAHINER
Department of Radiology, University of Michigan, Ann Arbor, Michigan

INTRODUCTION

X-ray mammography is the most sensitive diagnostic method for detecting early breast cancers. However, a mammogram is a two-dimensional projection of a three-dimensional (3-D) object. The anatomical structures along the x-ray beam path are projected onto an image plane and overlap each other, resulting in one of the major limitations in mammography—low sensitivity for detecting lesions overlapping with dense fibroglandular tissues (Jackson et al. 1993). It was estimated that about 20% of the breast cancers in dense breasts are not detected by mammography (Wallis et al. 1991, Bird et al. 1992). The camouflaging effect of the overlapping structures is the main cause of missed diagnoses. Stereoscopic imaging may allow overlying structures to be perceived at different depths, thereby reducing the camouflaging effect.

Stereoscopic imaging requires acquisition of two images. The x-ray focal spot is shifted, along a direction parallel to the image plane, to the left and the right of the central axis to obtain two images of the object. The object and the detector have to remain stationary during the process. The images are referred to as the left-eye and the right-eye images. When the two images are placed properly and viewed by trained eyes or with the aid of a stereoscope so that the left eye sees only the left-eye image and the right eye sees only the right-eye image, the parallax between the two images creates the depth perception. Stereoscopic radiography has been attempted for different types of examinations (Doi et al. 1981, Kelsey et al. 1982, Doi and Duda 1983, Higashida et al. 1988, Trocme et al. 1990, Ragnarsson and Karrholm 1992). Stereoscopic imaging has not achieved widespread acceptance in clinical practice however, mainly because of the doubled film cost and increased patient exposure (Curry et al. 1992). A secondary problem is the need to train the eyes to perceive the stereoscopic effect without aid, or to use a special stereoscope, with careful arrangement of the films. The recent advent of direct digital detectors may make the stereoscopic technique a viable approach because no additional film cost will be required. Furthermore, a digital detector has a wider linear-response range and a higher contrast sensitivity than a screen-film system so that good-quality images may be acquired at a reduced radiation dose. Images in digital form can be subjected to image processing, further enhancing the visibility of the image details. Digital stereoscopic images can be viewed on a single display device with the assistance of stereoscopic goggles providing an electronic shutter. The stereoscopic images can therefore be displayed singly in the conventional manner or stereoscopically on the same viewing station to provide complementary diagnostic information.

One of the advantages of stereoscopic imaging is the 3-D information it provides on the lesions of interest. It has been reported that the 3-D distribution of microcalcifications may be correlated with the malignant or benign nature of the cluster (Conant et al. 1996, Maidment et al. 1996). Spiculations from a mass may also be more readily distinguished from overlapping tissues under stereoscopic viewing conditions. The additional diagnostic information may improve the classification of malignant and benign lesions, thereby reducing unnecessary biopsies and increasing the positive predictive value of mammography.

The usefulness of stereomammography depends on the depth perception of subtle mammographic features. The amount of stereoscopic shift has to match the imaging geometry in order to achieve the best depth perception. The signal-to-noise ratio of mammographic features is determined mainly by the x-ray imaging techniques used. In this study, we evaluated the effects of imaging parameters on depth discrimination in stereomammographic imaging.

MATERIALS AND METHODS

Phantom Design

We have designed a modular stereo phantom for this study. The phantom contains six 1-mm-thick Lexan™ sheets, each separated by 1-mm-thick spacers. Each Lexan plate contains a 5 × 5 array of object areas. Fifty nylon fibrils, each about 8 mm in length and 0.53 mm in diameter, are arranged in these object areas. Twenty-five fibrils are oriented vertically (perpendicular) and 25 horizontally (parallel) to the stereo shift direction. The fibrils are placed in the object areas on the six Lexan plates such that, in the projection image, each object area contains the projection of one vertical and one horizontal fibril that cross each other. The depth separation of each pair of crossing fibrils depends on the arrangement of the plates. These plates can be randomly ordered to produce many independent object configurations. In this study, the phantom with a 1-mm-thick cover plate (total thickness of Lexan in phantom = 7 mm) was sandwiched in the middle of 4-cm-thick BR-12 breast-tissue-equivalent material to simulate the scatter condition for an average breast.

Image Acquisition and Display

Digital stereoscopic image pairs were acquired with a Fischer Mammotest stereotaxic prone biopsy table. The system acquires digital images of 1024 × 1024 pixels and 12 bit gray levels in a 5 cm × 5 cm field of view using a fiber-optics-coupled charged-coupled device (CCD) detector. No antiscatter grid is used with the digital detector. For this system, the automatic exposure technique at 26 kVp for a 4.2-cm-thick Lucite™ phantom is about 160 mAs. We acquired stereoscopic

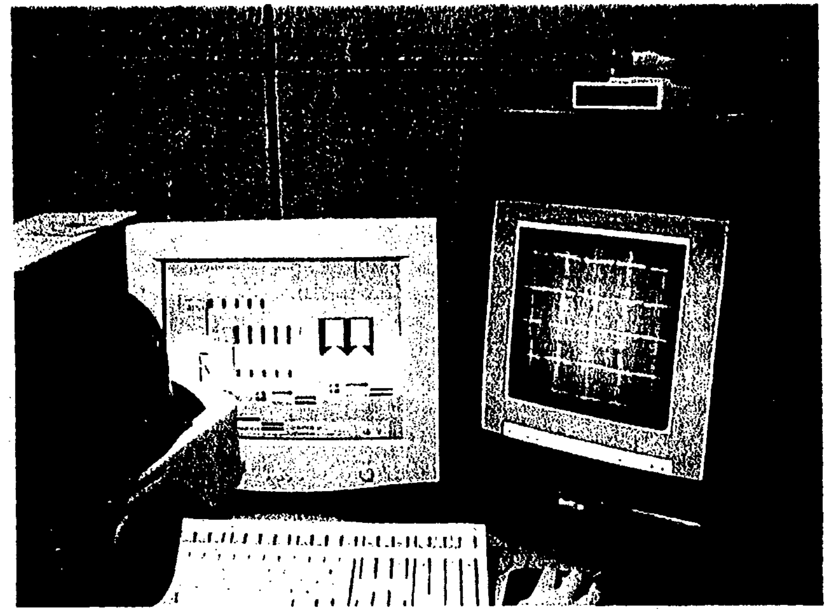

Figure 1. Stereoscopic display workstation.

pairs of images at ±2.5° and ±5° stereo-angles using 26 kVp and 40, 70, 140 mAs per image. Three different configurations of the fibril phantoms were imaged under each exposure condition, producing 75 pairs of fibril images at 5 different depth separations under each condition. A training image was also acquired at 26 kVp and 10 mAs without the 4 cm BR-12 phantom.

The images were displayed on a 21" Barco-Metheus (Beaverton, OR) display monitor driven by a model 1760S stereoscopic board and a SUN Microsystems (Palo Alto, CA) Ultra 10 computer. The Metheus board displays 1408 × 1408 × 8 bit images at a refresh rate of 114 Hz. It operates in a page flipping stereoscopic mode with the left- and right-eye images displayed alternately. NuVision (Beaverton, OR) LCD stereoscopic glasses were used for viewing the stereoscopic images. Figure 1 shows the stereoscopic display workstation used in this study.

Observer Experiment

Nine observers participated in the experiment. A total of 18 stereoscopic image pairs (2 stereo-angles × 3 exposure levels × 3 phantom configurations) were viewed by each observer. Each image contained 25 crossing pairs of fibrils separated by one of five different spacings (2, 4, 6, 8, 10 mm). The observer was asked to visually judge if the vertical fibril in each pair of overlapping fibrils was in front of or behind the horizontal fibril. Each observer read the 18 images sequentially in a different pre-assigned randomized order. The reading orders of the observers were chosen so that, on average, no image acquired under a specific condition would be read more frequently in a certain order. This minimized the effects of observer learning, memorization, or fatigue on the reading results. The observer was not informed of the conditions under which the image being viewed was acquired. The training image was read before the experiment by each observer to familiarize him or her with the reading task.

RESULTS

It was found that the stereovision of the observers differed by a wide range and it appeared to depend on the quality of the stereoscopic images. All observers could perceive the stereoscopic training image with reasonable accuracy in judging the relative depths of the crossing fibrils. The fibrils in the training image had a higher contrast and signal-to-noise ratio than the test images. It was acquired without the 4 cm BR-12 phantom so that the scattered radiation was much lower than that in the test images. Some observers found it much more difficult to merge the left-eye and right-eye images to achieve a stereoscopic effect when they viewed the test images. This occurred more often with the images acquired at ±5° stereo-angle than those acquired at ±2.5° stereo-angle. One of the observers failed to merge the images at the ±5° stereo-angle so that the results at this angle were analyzed for only eight observers.

Figures 2(a)–(d) show the percentages of correct decisions plotted as a function of the depth separation of the crossing fibrils, averaged over 9 (±2.5°) or 8 (±5°) observers, for the different imaging conditions studied. Because of the large variation in the accuracy of the observers, the standard deviations of the mean were large, ranging from 4% to 13%. The differences in the percentages of correct decisions between the different conditions were therefore not statistically significant. However, some trends can be observed. The curve for the highest exposure, 140 mAs, tended to be slightly higher than those for the other two exposures, except for a few points. The 140 mAs curves were also smoother than the other curves, indicating less variability in the readings. At this exposure level, the percentages of correct decisions appeared to increase by about 15% to 20% as the depth separation increased from 2 mm to 10 mm, and increase by an average of about 5% as the stereo-angle increased from ±2.5° to ±5°, when other conditions were fixed. The percentages of correct decisions were 10% to 15% higher when the vertical fibrils were in front of the horizontal fibrils than when they were in the back.

Three of the observers had a higher accuracy in depth discrimination than the others. On average, their percentages of correct decisions were about 10% to 20% higher than the other six observers under most conditions, and were 40% to 50% higher in some cases. For these observers, it is more obvious that the accuracy was higher when the vertical fibrils were in front of the horizontal fibrils. For the smallest fibril separation of 2 mm, the accuracy was about 20% higher when the vertical fibril was in the front.

CONCLUSION

This study shows that depth discrimination in stereomammography depends on imaging conditions and object configurations. For viewing of fibrils that simulated spiculations or thin fibrous structures in mammographic images, the

BEST AVAILABLE COPY

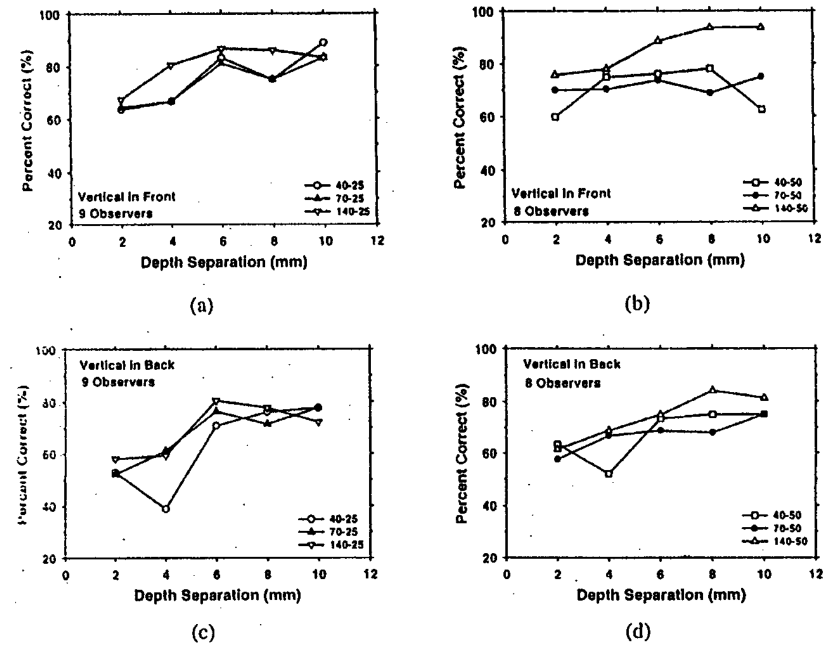

Figure 2. Dependence of percentage of correct decisions, averaged over 9 (±2.5°) or 8 (±5°) observers, on depth separation and imaging conditions: (a) vertical fibril in front, ±2.5° stereo-angle, (b) vertical fibril in front, ±5° stereo-angle, (c) vertical fibril in back, ±2.5° stereo-angle, and (d) vertical fibril in back, ±5° stereo-angle. 40 mAs, 70 mAs, 140 mAs were used for image acquisition.

accuracy of depth discrimination appeared to increase with increasing exposure and stereo-angle. However, many observers found it difficult to merge the left-eye and right-eye images acquired with a large stereo-shift to achieve stereovision. Further studies will be conducted to evaluate the depth perception of different mammographic test objects. Studies are also underway to evaluate if specially designed cursors can assist in depth discrimination and measurement of absolute depths of target objects in stereoscopic images (Goodsitt et al. 2000, 2001).

ACKNOWLEDGMENTS

This work is supported by U. S. Army Medical Research and Materiel Command Grant DAMD 17-98-1-8210. The content of this publication does not necessarily reflect the position of the funding agency, and no official endorsement of any equipment and product of any companies mentioned in this publication should be inferred.

BEST AVAILABLE COPY

REFERENCES

Bird, R. E., T. W. Wallace, and B. C. Yankaskas (1992). "Analysis of cancers missed at screening mammography." *Radiol.* 184: 613–617.

Conant, E. F., A. D. Maidment, M. Albert, C. W. Piccoli, S. A. Nussbaum, and P. A. McCue (1996). "Small field-of-view digital imaging of breast calcifications: method to improve diagnostic specificity." *Radiol.* 201(P): 369.

Curry, T. S., J. E. Dowdey, and R. C. Murry. *Christensen's Physics of Diagnostic Radiology*. Fourth ed. Philadelphia: Lea & Febiger. 1992.

Doi, K., and E. E. Duda (1983). "Detectability of depth information by use of magnification stereoscopic technique in cerebral angiography." *Radiol.* 146: 91–95.

Doi, K., N. J. Patronas, E. E. Duda, E. Geldner, and K. Dietz (1981). "X-ray imaging of blood vessels to the brain by use of magnification stereoscopic technique." *Advance Neurol.* 30: 175–189.

Goodsitt, M. M., H. P. Chan, and L. M. Hadjiiski (2000). "Stereomammography: Evaluation of depth perception using a virtual 3D cursor." *Med. Phys.* (in press).

Goodsitt, M. M., H. P. Chan, J. M. Sullivan, K. L. Darner, and L. M. Hadjiiski. "Evaluation of the Effect of Virtual Cursor Shape on Depth Measurements in Digital Stereomammograms" in *IWDM 2000, 5th International Workshop on Digital Mammography*. Martin Yaffe (ed.). IWDM Proceedings Toronto, Canada, June 11-14, 2000. Madison, WI: Medical Physics Publishing, pp. 45–50, 2001.

Higashida, Y., Y. Hirata, R. Saito, S. Doudanuki, H. Bussaka, and M. Takahashi (1988). "Depth determination on stereoscopic digital subtraction angiograms." *Radiol.* 168: 560–562.

Jackson, V. P., R. E. Hendrick, S. A. Feig, and D. B. Kopans (1993). "Imaging of the radiographically dense breast." *Radiol.* 188: 297–301.

Kelsey, C. A., R. D. Moseley, S. A. Mettler, and D. E. Briscoe (1982). "Cost-effectiveness of stereoscopic radiographs in detection of lung nodules." *Radiol.* 142: 611–613.

Maidment, A. D. A., M. Albert, E. F. Conant, C. W. Piccoli, and P. A. McCue (1996). "Prototype workstation for 3-D diagnosis of breast calcifications." *Radiol.* 201(P): 556.

Ragnarsson, J. I., and J. Karrholm (1992). "Factors influencing postoperative movement in displaced femoral neck fractures: Evaluation by conventional radiography and stereoradiography." *J. Orthop. Trauma* 6: 152–158.

Trocme, M. C., A. H. Sather, and K. N. An (1990). "A biplanar cephalometric stereoradiography technique." *Am. J. Orthodont. Dentofacial Orthoped.*98: 168–175.

Wallis, M. G., M. T. Walsh, and J. R. Lee (1991). "A review of false negative mammography in a symptomatic population." *Clin. Radiol.* 44: 13–15.

BEST AVAILABLE COPY

Measurement of Light Propagation Characteristics in a Gradient Gd_2O_2S Screen

VIRGIL N. COOPER, III
JOHN M. BOONE
J. ANTHONY SEIBERT
Department of Radiology, University of California Davis, Sacramento, California

WERNER ROECK
University of California Irvine, Irvine California

INTRODUCTION

The rationale for placing the film on the x-ray tube side of the scintillating screen within a mammographic film-screen cassette is well known. For digital mammographic systems, however, current technology does not permit the optical receptor to be positioned on the incident side of the scintillator. In order to design a screen with optimal resolution and absorption efficiency characteristics for digital mammography, one must have a fundamental understanding of the primary and secondary information carrier behavior in the screen. In this study, we complement theoretical studies existing in the literature (Nishikawa and Yaffe 1990, Lubberts 1968) by presenting an experimental approach to measuring these characteristics with use of a Gd_2O_2S gradient screen that has variable thickness along one dimension.

THEORY

This section describes a hypothetical experiment and demonstrates the approach and analysis techniques of this study. Consider a scintillating screen with increasing mass thickness from its edge to its center. Let the gradient screen be enclosed in a cassette with the film residing beneath the screen. A narrow x-ray beam defined by a slit perpendicularly oriented to the gradient is used to expose the cassette at incremental locations. This could be achieved by fixing the slit with respect to the x-ray beam and placing the cassette on a precision positioning track and subsequently moving that cassette in small increments for each exposure.

It is expected that if the x-ray beams are held to constant intensity as the cassette is imaged from the thin to the thick portion of the gradient screen, the subsequent processed film would have darkening line spread functions (LSFs) corresponding to the increasing absorption efficiency. If the thicker portions of the screen could be made excessively thick and that cassette were imaged in the same manner, the subsequent processed film would at first have darkening LSFs corresponding to the increased absorption efficiency of the screen and then lightening LSFs due to attenuation of optical photons within the screen. Finally, for an infinitely thick portion of the screen, the absorption efficiency would be 100%, but the optical photons would not propagate through the remaining resolution and DQE losses and study the performance of other direct conversion detector materials, such as gallium arsenide, selenium, and lead iodide, that could have desirable properties for this application. We are convinced that the development of new direct conversion detectors will lead to an improved SNR. In turn, this should provide an improvement in the detection and diagnosis of breast cancer.

REFERENCES

Dainty, J. C., and R. Shaw. *Image Science.* Academic Press, 1974.

Fujita, H., D. Y. Tsai, T. Itoh, K. Doi, J. Morishita, K. Ueda, and A. Oktsuka. "A simple method for determining the modulation transfer function in digital radiography." *IEEE Trans. Med. Imaging.* 11: 34–39.

Haus, A. G. "Screen-film Image Receptors and Film Processing" in *Syllabus: A Categorical Course in Physics—Technical Aspects of Breast Imaging.* A. G. Haus and M. J. Yaffe (eds.). RSNA, 85-101. Radiological Society of North America, 1994.

Judy, P. F. (1976). "The line spread function and modulation transfer function of a computed tomographic scanner." *Med. Phys.* 3: 233–236.

Knoll, J. F. *Radiation Detection and Measurement.* 2nd ed. John Wiley & Sons, 1989.

Mainprize, J. G., N. L. Ford, S. Yin, T. Tümer, and M. J. Yaffe (2000). "Image quality of a prototype direct conversion detector for digital mammography." *Proc. SPIE.* In Press.

BEST AVAILABLE COPY

Evaluation of the Effect of Virtual Cursor Shape on Depth Measurements in Digital Stereomammograms

MITCHELL M. GOODSITT
HEANG-PING CHAN
JEFFREY M. SULLIVAN
LATIE L. DARNER
LUBOMIR M. HADJIISKI
Department of Radiology, University of Michigan, Ann Arbor, Michigan

INTRODUCTION

The superposition of tissues is a major problem in conventional mammograms. It can result in the camouflaging of masses within dense tissues. It can also lead to false positive mass detection wherein objects that appear mass-like are formed by superimposed structures. The superposition problem can be reduced or eliminated by generating and viewing three-dimensional (3-D) mammograms via techniques such as stereomammography.

Stereomammography was first described in 1930 (Warren 1930). It involved taking two separate mammograms, one at an x-ray tube angle of about +3° relative to the central axis, and the other at an angle of about −3°. These films were then viewed using special devices that employed mirrors or prisms to send one image to the observer's left eye and the other to the observer's right eye. Because this methodology required taking two films in roughly the same projection, it had several disadvantages including increased x-ray dose, expense, processing time, technologist time, and radiologist viewing time. These disadvantages of film stereomammography eventually outweighed the 3-D visualization advantage, and film stereomammography was discontinued.

Today's digital mammography machines eliminate or reduce most of the disadvantages, thereby making digital stereomammography a potentially viable technique. In particular, the linear response of the digital detectors makes it possible to utilize half the normal dose for each image. The observer's eye-brain system integrates the two images of the stereo pair to yield about the same signal-to-noise ratio as in a single image taken with the same total dose. Image processing and display are almost instantaneous, and viewing the images on a television monitor with LCD (liquid-crystal display) glasses that are synchronized so the left eye sees one image and the right the other is convenient and less time consuming than the film counterpart.

We have been employing a small field-of-view digital mammography system to investigate a new technique that is made possible through the integration of computer graphics with the stereoscopic image display. We generated a virtual 3-D cursor that can be calibrated to measure the depths of objects in digital stereomammograms. In our first studies, we investigated the accuracies of observers' measurements of the depths of horizontally and vertically oriented nylon filaments that simulated fibrils in mammograms (Goodsitt et al. 2000). We found that with a cross-shaped cursor, observers could measure depths of vertically oriented fibrils to 1 to 2 millimeters (mm), but their accuracies were degraded for horizontally oriented fibrils. The purpose of the present study was to investigate whether the depth accuracy of the horizontally oriented fibrils might be improved through the use of a specially designed cursor.

MATERIALS AND METHODS

We employed the images that were generated for our previous study (Goodsitt et al. 2000). These images were obtained with a Fischer (Denver, CO) MammoVision Stereotaxic unit using a stereo x-ray tube shift angle of −2.5° to +2.5°. The phantom that was imaged consisted of six 1-mm thick Lexan sheets each separated by 1-mm spacers. A matrix of 8-mm long, 0.53 mm diameter nylon fibrils was placed on the plates with 25 fibrils oriented vertically (perpendicular) and 25 horizontally (parallel) to the stereo shift direction. The depths and orientations of the fibrils were randomized and organized such that one horizontal fibril crossed one vertical fibril at each of the 25 matrix positions. The order of the Lexan layers could be changed to create many independent phantom configurations. A photograph of the phantom appears in figure 1.

A commercial stereoscopic display with a cross-shaped virtual cursor (Neotek, Inc, Pittsburgh, PA) was employed in our previous study. This display utilizes a synch-doubling method to achieve stereo imaging at twice the normal refresh rate of a display monitor, thereby minimizing flicker. This is a relatively inexpensive method for displaying high-quality stereoscopic images. Its primary disadvantage is that it involves the storage of the left eye image above the right

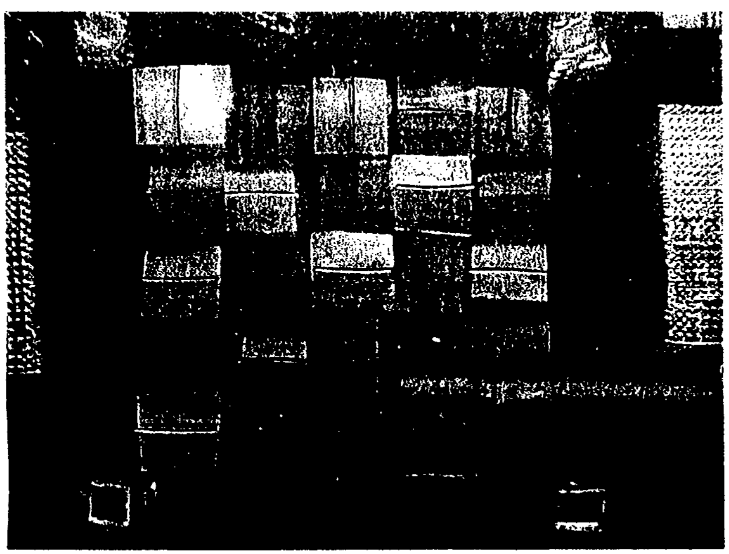

Figure 1. Front-view photograph of the phantom that was imaged.

BEST AVAILABLE COPY

eye image in the computer frame buffer, and in order to accomplish this with most frame buffers, the vertical resolution of both images must be reduced by about a factor of two (e.g., two 1024 × 1024 images must each be reduced to about 1024 × 380 to fit in a 1024 × 768 frame buffer). For the present study, we developed software to display images and to generate cursors of user-selected shapes on a high-end stereoscopic display/viewing system. A Barco-Metheus (Beaverton, OR) model 1760S stereoscopic board was employed in a SUN Microsystems (Palo Alto, CA) Ultra 10 computer. The Metheus board operates in a page-flipping stereoscopic mode whereby the full left and right eye images are displayed sequentially, one after the other. This board is capable of displaying 1408 × 1408 × 8 bit images at a refresh rate of 114 Hz. The images in our study were displayed on a 21" Barco monitor and viewed with NuVision (Beaverton, OR) LCD stereoscopic glasses.

Software was written to allow the user to design and display virtual (stereoscopic) cursors and to display the x, y, and z positions of those cursors. The 3-D nature of the cursor is achieved by introducing offsets in the horizontal positions of the representations of the cursor in the left and right eye images. The z-coordinate is equal to the offset. When the offset is 0, the cursor is at the same x, y position in both images, and it appears stereoscopically to be at the depth of the monitor screen. As the horizontal offset between the cursor positions is increased in one direction (e.g., left), the cursor appears to move closer to the observer, and as the offset is increased in the opposite direction (e.g., right), the cursor appears to move toward or into the monitor. The z-coordinate was calibrated by imaging thin wires placed on the steps of a stepwedge with known step heights. The stepwedge was imaged with the Fischer MammoVision system using the same x-ray tube shift as for the images of the fibril phantoms. The wires that were employed for calibration were oriented perpendicular to the tube shift direction. The resulting stereoscopic images were viewed without the stereo glasses and the left and right eye cursor positions were adjusted to overlay the left and right eye images of the wires on the steps. The z-coordinates of the cursor were linearly fit to the known depths of the wires to obtain the calibration line.

For the observer experiment, we had each participant use the stereoscopic virtual cursor system to measure the depths of 25 horizontally oriented fibrils in each of two images (two different phantom configurations) for a total of 50 depth measurements per person. Each participant made these measurements twice using different cursors. One cursor was cross-shaped and the other was comb-shaped. The cursors are sketched in figure 2.

An artist's interpretation of the stereoscopic viewing apparatus appears in figure 3.

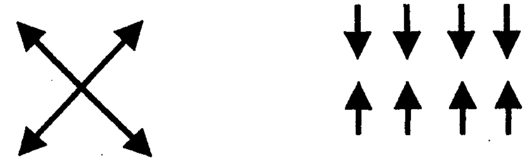

Figure 2. "Cross-shaped" and "fan-shaped" cursors employed in the experiment.

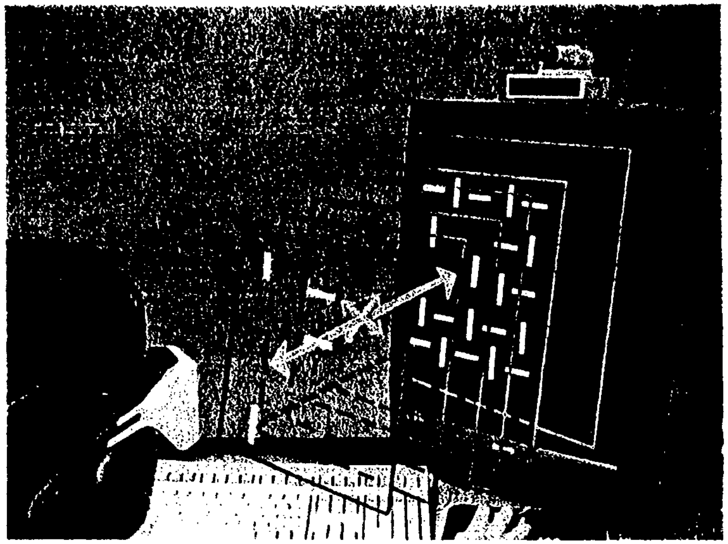

Figure 3. Graphical representation of the stereoscopic viewing system simulating the observer moving the virtual cursor within the stereo (3-D) image to match the horizontal fibril location.

The comb-shaped cursor was chosen because it provides the observer with more vertical depth cues. It was hoped that when the observer positioned the comb cursor such that the horizontal fibril appeared to move through the central slot as the cursor depth was varied, the additional depth cues might assist the observer in locating the depth of the fibril.

The observers recorded their measured z-coordinates of each horizontally oriented fibril, and these z-coordinates were converted to depths using the calibration line that was calculated from the stepwedge data discussed above. These depths were then compared with the known depths in terms of the parameters associated with least-square linear fits [slope, intercept, correlation coefficient (r-value), and standard error of the estimate (SEE)] of the measured depths to the true depths and in terms of the root mean square (RMS) errors of the measurements. The latter were computed using the equation:

$$RMS\ error = \sqrt{\frac{\sum_{i=1}^{50}(true\ depth_i - measured\ depth_i)^2}{50}}$$

RESULTS

The results of the experiment are summarized in table 1. Plots of the best and worst results are shown in figure 4.

Table 1. Linear Fit Parameters and RMS Errors for Measured vs. True Depths of Horizontally Oriented Fibrils

	Observer 1	Observer 1 Repeat	Observer 2	Observer 3	Observer 4
Slope (cross)	0.71	0.74	1.02	0.48	0.56
Slope (comb)	0.91	0.94	0.87	0.51	0.47
Intercept (cross)	0.44	1.09	−0.50	0.04	1.54
Intercept (comb)	0.79	0.63	0.75	1.94	1.11
r-value (cross)	0.80	0.83	0.94	0.55	0.48
r-value (comb)	0.98	0.97	0.95	0.60	0.49
SEE (cross) mm	1.70	1.58	1.20	2.32	3.28
SEE (comb) mm	0.64	0.72	0.95	2.16	2.68
RMS error (cross) mm	2.17	1.76	1.24	3.84	3.57
RMS error (comb) mm	0.76	0.80	0.98	2.68	3.50

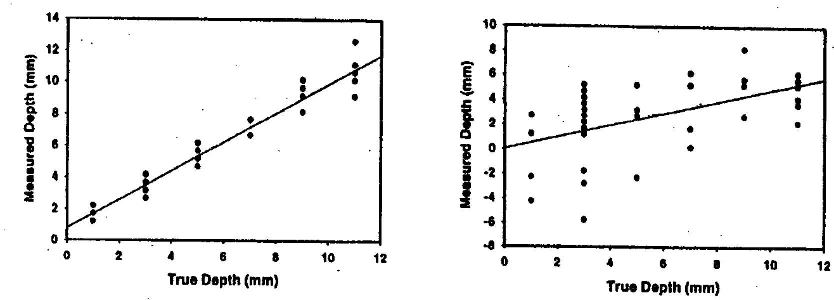

Figure 4. Left: Best measured vs. true depth result (observer #1, comb cursor). Right: Worst measured vs. true depth result (observer #3, cross cursor).

DISCUSSION

Depth measurements made with the new comb-shaped cursor were more accurate. The RMS errors in the observers' measurements improved by 0.1 to 1.4 mm with this cursor relative to the cross-shaped cursor. In fact, with this new cursor, two of the observers were able to measure the depths of the horizontally oriented fibrils to an accuracy of about 1 mm, which approaches their accuracies for the vertically oriented fibrils in our previous study (Goodsitt et al. 2000). One of the observers repeated the entire experiment twice and those results appear in table 1. The linear fit parameters and RMS errors for the two trials by the same observer are very similar, indicating the results for that observer are very reproducible. The accuracies of all of the observers' measurements that are listed in table 1 do not tell the whole story. They do not reflect the amount of time required to make the measurements. In general, observers spent much more time locating the positions of the horizontally oriented fibrils as compared with the vertically oriented fibrils. The observers would move the cursors in and out several times to hone in on the depths, which were much less obvious than the depths of the vertically oriented fibrils. The good results that were obtained indicate that the extra time and effort were worthwhile. Most objects in mammograms have orientations that are between horizontal and vertical, and even small vertical components make the depths easier to visualize and help reduce measurement times. We have designed an anthropomorphic breast phantom containing spiculated masses and microcalcification clusters at various known depths. In future studies, we will analyze the accuracies of depth measurements of the spiculations, microcalcifications, and masses in that phantom with virtual cursors of different shapes and sizes.

ACKNOWLEDGMENT

This work is supported by U. S. Army Medical Research and Materiel Command Grant DAMD 17-98-1-8210. The content of this publication does not necessarily reflect the position of the funding agency, and no official endorsement of any equipment and product of any companies mentioned in this publication should be inferred.

REFERENCES

Goodsitt, M., H.-P. Chan, and L. M. Hadjiiski (2000). "Stereomammography: Evaluation of depth perception using a virtual 3D cursor." Accepted for publication, *Medical Physics*.

Warren, S. L. (1930). "Roentgenologic study of the breast." *AJR* 24: 113–124.

Decreased Breast Compression Using Digital Mammography at Screen/Film Mean Glandular Dose

C. KIMME-SMITH
T.-Y. YEE
L. W. BASSETT
Radiological Sciences, University of California, Los Angeles, California

INTRODUCTION

Low energy x-rays are required in mammography to preserve soft tissue contrast. As a result, the breast must be compressed to thicknesses ranging from 2 cm to 8 cm so that x-ray penetration is possible. Compression of the breast also decreases the latitude needed by film, since thicker portions of the breast near the chest wall are reduced by compression. This has allowed film manufacturers to provide higher contrast film for mammography, thus amplifying soft tissue contrast even more. Another added benefit has been the decrease in scatter due to the shorter interaction path of each photon; compressed breast tissue is also spread out, thus reducing tissue overlap (Kimme-Smith et al. 1998). During the 1970's, xeromammography required less compression because it used a higher kVp than screen/film mammography in order to increase sensitivity of the selenium plates used as image receptors. Contrast was restored, or enhanced, by an edge effect produced by the electrostatic effect of the blue powder used to develop the latent image on the exposed selenium plates. When lower dose screen/film was introduced, and more compression was required during mammography, many women objected. Several radiologists responded to these complaints by questioning their mammography patients, and the results of surveys indicated that women did not avoid mammography because of breast compression (Jackson et al. 1988, Dullum et al. 2000). These questionnaire responses also showed that most women would prefer less compression and found mammography an uncomfortable procedure.

The advent of whole breast digital mammography has brought with it many questions about its usefulness. Is it merely a replacement for screen/film mammography, or will it bring added benefits in diagnostic accuracy? The ability to enhance displayed contrast in digital images may permit this modality to improve lesion visibility in the mammograms of difficult to image breasts that are not well served by screen/film mammography. This paper, however, explores another possible aspect of digital mammography. Since higher kVp techniques [but resulting in the same mean glandular dose (MGD)] have been shown to increase the signal to noise ratio in digitally acquired mammograms (Kimme-Smith et al. 1998), could we not increase kVp and also decrease compression in order to make mammography more comfortable for women? Potentially, the loss of subject contrast due to higher kVp techniques and decreased compression could be restored by contrast enhancement to achieve a diagnostic content equivalent to that of screen/film mammography. This paper describes the steps needed to begin such an experiment. First, women had to be questioned concerning what level of compression was comfortable for them. Then the available screen/film units in

Digital Stereomammography: Observer Performance Study of the Effects of Magnification and Zooming on Depth Perception

Heang-Ping Chan, Mitchell M. Goodsitt, Lubomir M. Hadjiiski, Janet E. Bailey, Katherine Klein, Katie L. Darner, Chintana Paramagul

Department of Radiology, University of Michigan, Ann Arbor, MI 48109

ABSTRACT

We have previously reported the effects of stereo angle and exposure on depth discrimination and the use of virtual cursors for absolute depth measurements in digital stereomammography. The current study further investigates the effects of magnification and zooming on depth perception. Stereoscopic image pairs of a phantom were acquired with a full-field digital mammography system. The modular phantom contained 25 crossing fibril pairs with depth separations between each pair ranging from 2 to 10 mm. Three phantom (fibril) configurations were imaged using techniques of 30 kVp, Rh/Rh, ±3° stereo angle, , contact and 1.8X magnification geometry, and 4 to 63 mAs exposure range . The images were displayed on a Barco monitor driven by a Metheus stereo graphics board and viewed with LCD stereo glasses. Five observers participated in the study. Each observer visually judged if the vertical fibril was in front of or behind the horizontal fibril in each pair. It was found that the accuracy of depth discrimination increased with increasing fibril depth separation and x-ray exposure. Zooming the contact stereo images by 2X did not improve the accuracy. Under conditions of high noise (low mAs) and small depth separation between the fibrils, depth discriminations were significantly better in stereo images acquired with geometric magnification than in images acquired with a contact technique and displayed with or without zooming. This study indicates that stereoscopic imaging, especially with magnification, may be useful for visualizing the spatial distribution of microcalcifications in a cluster and differentiating overlapping tissues from masses on mammograms.

KEY WORDS: Digital mammography, stereoscopic imaging, magnification, observer performance study.

1. INTRODUCTION

Mammography is the most sensitive method for detecting early breast cancers. However, because of the projection of the breast tissues along the x-ray beam path onto a two-dimensional image plane, one of the major limitations in mammography is the low sensitivity for detecting lesions overlapping with dense fibroglandular tissues[1]. It has been estimated that about 20% of breast cancers in dense breasts are missed [2, 3]. The camouflaging effect of overlapping structures is the main cause of missed diagnoses. New breast imaging techniques such as stereomammography[4-7], digital tomosynthesis[8, 9], and computed tomography[10] may alleviate this problem.

Stereoscopic imaging requires acquisition of two images. The x-ray focal spot is shifted, along a direction parallel to the image plane, to the left and the right of the central axis to obtain two images, referred to as the left-eye and the right-eye images, respectively, of the object. When the two images are placed properly and viewed so that the left eye sees only the left-eye image and the right eye sees only the right-eye image, the parallax between the two images creates the depth perception. Stereoscopic radiography has been attempted for different types of examinations but it has not achieved widespread acceptance in clinical practice, however, mainly because of the doubled film cost and increased patient exposure [11]. The recent advent of direct digital detectors may make the stereoscopic technique a viable approach because no additional film cost will be required. Furthermore, a digital detector has a wider dynamic range and higher contrast sensitivity than a screen-film system so that good-quality images may be acquired at a reduced radiation dose. Digital stereoscopic images can be viewed on a single display monitor with the assistance of stereoscopic goggles that provide an electronic shutter to show the left- and right-eye images to the respective eyes. The stereoscopic images can therefore be displayed singly in the conventional manner or stereoscopically on the same viewing station to provide complementary diagnostic information.

An advantage of stereoscopic imaging is the three-dimensional (3D) structural information that it provides for the lesions of interest. The 3D distribution of microcalcifications may be correlated with the malignant or benign nature of the cluster[12, 13]. Spiculations from a mass may also be more readily distinguished from overlapping tissues under stereoscopic viewing conditions. The additional diagnostic information may improve the classification of malignant and benign lesions, thereby reducing unnecessary biopsies. It has been reported that digital stereomammography allowed the detection of additional lesions that were obscured on screen-film mammograms[4].

We are investigating the usefulness of stereomammography for discriminating the depths of subtle mammographic features. We previously demonstrated that a virtual cursor could provide accurate depth measurements in stereo phantom images acquired under mammographic conditions[5, 6, 14]. We also studied the effects of stereo shift and imaging conditions on the depth perception of crossing fibrils in stereo phantom images[15]. In this study, we further evaluated the effects of geometric magnification, display zooming, and x-ray exposure on the visual depth discrimination of fibril-like objects in stereo phantom mammograms. The results of our observer performance study are discussed in this paper.

2. MATERIALS AND METHODS

2.1 Phantom Design

We have designed a modular stereo phantom for evaluation of the depth perception task. The phantom consists of six 1-mm-thick Lexan sheets, each separated by 1-mm-thick spacers. Each Lexan plate contains a 5 X 5 array of object areas. Fifty nylon fibrils, each about 8-mm in length and 0.53 mm in diameter, are arranged in these object areas. Twenty-five fibrils are oriented vertically (perpendicular) and 25 horizontally (parallel) to the stereo shift direction. The fibrils are placed in the object areas on the six Lexan plates such that, in the projection image, each object area contains the projection of one vertical and one horizontal fibril that cross each other. The depth separation of each pair of crossing fibrils depends on the arrangement of the plates. These plates can be arranged in different orders to produce many independent object configurations.

2.2 Image Acquisition and Display

Digital stereoscopic image pairs were acquired with a GE Senographe 2000D digital mammography system. The system employs a digital detector consisting of a CsI:Tl scintillator and an amorphous-Si active matrix flat panel. The detector measures 23 cm x 18 cm, with a pixel size of 100 μm x 100 μm. We acquired stereoscopic pairs of images using x-ray techniques of 30 kVp, Rh target/Rh filter, a ±3° stereo-angle, contact (reciprocating grid, 0.3 mm focal spot) and 1.8X magnification (no grid, 0.15 mm focal spot) geometies, and exposures of 4, 8, 32, and 63 mAs per image. Three different configurations of the fibril phantoms were imaged under each exposure condition. Twenty-four stereo image pairs were thus produced. For each exposure/geometry condition, there were a total of 75 pairs of fibril images (25 fibril pairs in each phantom configuration x 3 configurations) at 5 different depth separations (2, 4, 6, 8, 10 mm) to be evaluated.

The images were displayed on a 21" Barco-Metheus (Beaverton, OR) model 521 display monitor driven by a model 1760S stereoscopic board and a SUN Microsystems (Palo Alto, CA) Ultra 10 computer. The Metheus board displays 1408 x 1408 x 8 bit images at a refresh rate of 114 Hz . It operates in a page flipping stereoscopic mode with the left- and right-eye images displayed alternately. NuVision (Beaverton, OR) LCD stereoscopic glasses were used for viewing the stereoscopic images.

2.3 Observer Experiment

Five observers including two experienced mammographic radiologists participated in the experiment. The contact images were read in two modes – a regular and a 2X-zoom mode. The 1.8X geometric magnification images were read only in the regular mode. The observers were asked to visually judge if the vertical fibril in each pair of overlapping fibrils was in front of or behind the horizontal fibril. Each observer read the images sequentially in a different randomized order. The observers were not informed of the conditions under which the image being viewed was acquired. Prior to reading the test cases, the observers participated in training sessions to become familiar with the reading task.

3. RESULTS

Tables 1-3 summarize the percentages of correct decisions on the relative depths as a function of the depth separation of the crossing fibrils, averaged over 5 observers, for the different exposure levels studied. The statistical significance (two-tailed p level<0.05) of the differences between every two conditions: contact and contact-zoom, contact and magnification, and contact-zoom and magnification was estimated by a paired-t test. The t-test was performed for each depth separation and exposure level over the 5 observers. It was found that the differences between the contact and contact-zoom viewing conditions were not statistically significant. The differences between the contact and magnification geometries were statistically significant for depth separations of 2 mm to 6 mm at 4 mAs, and for 2-mm separation at 8 mAs. The differences between the contact-zoom and magnification were statistically significant for depth separations of 2 mm to 6 mm at 4 mAs, for 2-mm to 4-mm separations at 8 mAs, and for 2-mm separation at 32 mAs.

Table 1. The average percentage of correct decision in differentiating the depths of two crossing fibrils in stereo images acquired with contact geometry and displayed without zooming.

Depth Separation (mm)	Exposure			
	4 mAs	8 mAs	32 mAs	64 mAs
2	68.8	77.6	87.2	92.0
4	76.7	94.4	97.8	96.7
6	90.0	98.3	100.0	100.0
8	95.3	98.8	97.6	100.0
10	100.0	100.0	100.0	100.0

Table 2. The average percentage of correct decision in differentiating the depths of two crossing fibrils in stereo images acquired with contact geometry and displayed with 2X zoom.

Depth Separation (mm)	Exposure			
	4 mAs	8 mAs	32 mAs	64 mAs
2	72.8	83.2	89.6	93.6
4	81.1	91.1	98.9	100.0
6	83.3	98.3	100.0	100.0
8	91.8	96.5	96.5	100.0
10	100.0	100.0	100.0	100.0

Table 3. The average percentage of correct decision in differentiating the depths of two crossing fibrils in stereo images acquired with 1.8X magnification geometry and displayed without zooming.

Depth Separation (mm)	Exposure			
	4 mAs	8 mAs	32 mAs	64 mAs
2	92.0	93.6	97.6	98.4
4	98.9	100.0	100.0	100.0
6	98.3	100.0	100.0	100.0
8	100.0	98.8	100.0	100.0
10	100.0	100.0	100.0	100.0

4. CONCLUSIONS

This study shows that the accuracy of depth discrimination of fibrils in stereomammography increases with x-ray exposure and depth separation and depends on imaging geometry. Depth discrimination at ±3° stereo angle was reasonably good, 2-mm depth resolution was achieved with over 60% accuracy for all imaging conditions studied. It improved to greater than 90% accuracy at higher doses and contact geometry. Under our experimental conditions, zooming the contact stereo images by 2X did not improve the accuracy. When the images were noisy and the depth separation between the fibrils was small, depth discriminations were significantly better in stereo images acquired with geometric magnification than in images acquired with a contact technique and displayed with or without zooming. Magnification stereomammography provided over 90% accuracy at 2-mm depth resolution for all exposure levels studied. These results indicate that stereoscopic imaging, and in particular, magnification stereomammography, may be useful for visualizing the spatial distribution of microcalcifications in a cluster and differentiating overlapping tissues from masses on mammograms. Further studies are underway to evaluate use of other stereo angles (e.g., ±6°) and to investigate if specially designed cursors can assist in depth discrimination and measurement of absolute depths of target objects in stereoscopic images[5, 6, 14].

ACKNOWLEDGMENTS

This work is supported by U. S. Army Medical Research and Materiel Command Grants DAMD 17-98-1-8210 and DAMD17-99-1-9294. The content of this publication does not necessarily reflect the position of the funding agency, and no official endorsement of any equipment and product of any companies mentioned in this publication should be inferred.

REFERENCES

1. V. P. Jackson, R. E. Hendrick, S. A. Feig and D. B. Kopans, "Imaging of the radiographically dense breast," Radiology 188, 297-301 (1993).
2. R. E. Bird, T. W. Wallace and B. C. Yankaskas, "Analysis of cancers missed at screening mammography," Radiology 184, 613-617 (1992).
3. M. G. Wallis, M. T. Walsh and J. R. Lee, "A review of false negative mammography in a symptomatic population," Clinical Radiology 44, 13-15 (1991).
4. D. J. Getty, R. M. Pickett and C. J. D'Orsi, "Stereoscopic digital mammography: improving detection and diagnosis of breast cancer," Computer Assisted Radiology and Surgery 2001, Proceedings of the 15th International Congress and Exhibition, Berlin, International Congress Series 1230, 506-511 (2001).
5. M. M. Goodsitt, H. P. Chan and L. M. Hadjiiski, "Stereomammography: Evaluation of depth perception using a virtual 3D cursor," Medical Physics 27, 1305-1310 (2000).
6. M. M. Goodsitt, H. P. Chan, J. M. Sullivan, K. L. Darner and L. M. Hadjiiski, "Evaluation of the effect of virtual cursor shape on depth measurements in digital stereomammograms," The 5th International Workshop on Digital Mammography, Toronto, Canada, Proc. IWDM-2000, 45-50 (2000).
7. H. P. Chan, M. M. Goodsitt, K. L. Darner, J. M. Sullivan, L. M. Hadjiiski, N. Petrick and B. Sahiner, "Effects of stereoscopic imaging technique on depth discrimination," The 5th International Workshop on Digital Mammography, Toronto, Canada, Proc. IWDM-2000, 13-18 (2000).
8. L. T. Niklason, B. T. Christian, L. E. Niklason, D. B. Kopans, D. E. Castleberry, B. H. Opsahl-Ong, C. E. Landberg, P. J. Slanetz et. al., "Digital tomosynthesis in breast imaging," Radiology 205, 399-406 (1997).
9. S. Suryanarayanan, A. Karellas, S. Vedantham, S. P. Baker, S. J. Glick, C. J. D'Orsi and R. L. Webber, "Evaluation of linear and nonlinear tomosynthetic reconstruction methods in digital mammography," Academic Radiology 8, 219-224 (2001).
10. J. M. Boone, T. R. Nelson and J. A. Seibert, "The potential for breast CT," Medical Physics 28, 1246 (abstract) (2001).
11. T. S. Curry, J. E. Dowdey and R. C. Murry, *Christensen's Physics of Diagnostic Radiology.*, Fourth ed. (Lea & Febiger, Philadelphia, PA, 1992).
12. A. D. A. Maidment, M. Albert, E. F. Conant, C. W. Piccoli and P. A. McCue, "Prototype workstation for 3-D diagnosis of breast calcifications," Radiology 201(P), 556 (1996).
13. E. F. Conant, A. D. Maidment, M. Albert, C. W. Piccoli, S. A. Nussbaum and P. A. McCue, "Small field-of-view digital imaging of breast calcifications: method to improve diagnostic specificity," Radiology 201(P), 369 (1996).
14. M. M. Goodsitt, H. P. Chan, K. L. Darner and L. M. Hadjiiski, "The effects of stereo shift angle, geometric magnification, and display zoom on depth measurements in digital stereomammography," Medical Physics (submitted) (2002).
15. H. P. Chan, M. M. Goodsitt, J. M. Sullivan, K. L. Darner and L. M. Hadjiiski, "Depth perception in digital stereoscopic mammography," Poster presentation at the Era of Hope Meeting, U. S. Army Medical Research and Materiel Command, Department of Defense, Breast Cancer Research Program, Atlanta, Georgia, (2000).

AbstractID: 9572 Title: ROC Study Comparing Radiologists' Performances in Evaluating Breast Lesions on Stereoscopic and Single-Projection Digital Specimen Mammograms

We are evaluating the effects of stereoscopic imaging on the interpretation of mammographic lesions. For the present investigation, we conducted an observer ROC study to compare radiologists' performance in characterizing breast lesions in biopsy tissue specimens from stereo and single-projection digital mammograms. Stereo and single-projection images of 158 tissue specimens were acquired with a GE 2000D digital mammography system. The images were displayed on a DOME/MegaScan stereo display system and viewed with LCD glasses. A graphical user interface was developed that allowed the user to adjust the image display parameters and to record the BI-RADS assessment and confidence ratings on the presence of microcalcifications and masses, margin clearance, and likelihood of malignancy. A preliminary study was conducted with two MQSA radiologists. For one observer, the viewing of stereo images resulted in improvements in the accuracy of estimating the likelihood of malignancy (from Az= 0.72 to 0.74) and BI-RADS assessment (from Az= 0.68 to 0.73), and increased confidence in judging margin clearance ($p<0.00001$). For the other observer, the effect was the opposite - reduced accuracy in estimating the likelihood of malignancy (from Az= 0.76 to 0.70), reduced BI-RADS assessment (from Az= 0.77 to 0.72) and reduced confidence in judging margin clearance ($p<0.03$). These results appear to indicate that characterization of the lesions is correlated with the observer's confidence in visualizing the details in the stereo images, which may be affected by the observer's stereo acuity. The observer study will continue with additional radiologists, and the results will be presented.

DEVELOPMENT OF DIGITAL STEREO IMAGING TECHNIQUE FOR MAMMOGRAPHY

Heang-Ping Chan, Mitchell Goodsitt, Lubomir Hadjiiski, Mark Helvie, Janet Bailey, Katherine Klein, and Marilyn Roubidoux

Department of Radiology, University of Michigan, Ann Arbor, MI 48109

chanhp@umich.edu

One of the limitations of mammographic imaging is that overlapping dense tissue in the breast can camouflage true lesions or create false lesions in the projected image. The goal of this project is to develop a digital stereoscopic imaging technique for mammography. It is expected that overlying dense tissues will be separated from the lesion in the stereoscopic views, thereby increasing the conspicuity of the lesion, and that the ability to analyze the 3-dimensional (3D) distributions and shapes of lesions such as calcifications and masses can potentially improve the accuracy of mammographic interpretation by radiologists and reduce unnecessary biopsies.

We have investigated the dependence of depth discrimination on imaging parameters including the stereo angle, x-ray exposure, magnification, and display zoom. Image display software was developed for a high-quality stereo viewing station. Observer studies were conducted to view stereo images of 3D mammographic phantoms acquired under various imaging conditions. The accuracy of the observers in differentiating the relative depths of two overlapping fibrils was evaluated. In addition, we have developed 3D virtual cursors for measurement of the depth of objects in a stereomammogram. The effects of imaging parameters and virtual cursor shapes on depth measurement accuracy have been studied.

It was found that the accuracy of depth discrimination increased with increasing stereo angle, exposure, and fibril depth separation. Zooming the contact stereo images by 2X did not improve the accuracy. Under conditions of high noise and small depth separation between the fibrils, depth discrimination was significantly better in stereo images acquired with geometric magnification than in images acquired with a contact technique and displayed with or without zooming. Magnification mammography also provided the highest accuracy for depth measurement with a virtual cursor, whereas display zoom did not improve accuracy.

These studies indicate that stereoscopic imaging, especially with magnification, may be useful for differentiating overlapping tissues from masses on mammograms and visualizing the spatial distribution of microcalcifications in a cluster, thereby improving the accuracy of mammography for breast cancer detection and diagnosis.

Original work supported by the U.S. Army Medical Research and Materiel Command under DAMD17-98-1-8210.